ENHANCING SELECTIVE DECOMPOSITION OF IBUPROFEN ONTO POROUS TiO_2 NANOPARTICLES

by

ABOLFAZL ZAKERSALEHI

Presented to the Faculty of the Graduate School of

The University of Texas at Arlington in Partial Fulfillment

of the Requirements

for the Degree of

MASTER OF SCIENCE IN ENVIRONMENTAL ENGINEERING

THE UNIVERSITY OF TEXAS AT ARLINGTON

May 2013

Copyright © by Abolfazl Zakersalehi 2013

All Rights Reserved

ACKNOWLEDGEMENTS

I would like to express my sincere gratitude to my advisor, Dr. Hyeok Choi, for his continuous motivation and support and especially for his outstanding scientific guidance during my master degree. I would also like to thank Dr. Andrew Kruzic and Dr. Melanie L. Sattler for serving my committee and their valuable advices and criticisms.

I would also like to thank the following organizations and individuals for supporting my graduate research and studies through awards, assistantship and scholarship: University of Texas at Arlington (Department of Civil and Environmental Engineering), American Chemical Society (Division of Environmental Chemistry).

I sincerely appreciate the collaborations with my lab mates throughout my research period: Dr. Prince A. Nfodzo, Wasiu Lawal and Hesam Zamankhan Malayeri.

April 17, 2013

ABSTRACT

ENHANCING SELECTIVE DECOMPOSITION OF

IBUPROFEN ONTO POROUS TiO_2

NANOPARTICLES

Abolfazl Zakersalehi M.S.

The University of Texas at Arlington, 2013

Supervising Professor: Hyeok Choi

Advanced oxidation technologies have gained tremendous attention for water treatment purposes after demonstration of insufficient efficiency of conventional systems for removal of many emerging chemicals of concern. Among AOTs, a TiO_2-UV system is one of the most promising approaches due to its green properties and its effectiveness in generation of extremely oxidizing species such as hydroxyl radicals. However it has been demonstrated that non-selectivity of HRs in decomposition of organic compounds results in parallel decomposing of naturally abundant organic matter (NOM) along with toxic target contaminant, which significantly decreases the decomposition rate of target contaminants.

Despite a great amount of researches conducted on TiO_2 photocatalysts, limited success has been achieved in enhancing selectivity of TiO_2 photocatalytic oxidation.

In this study. a novel approach for suppressing the adverse effect of co-existing organics such as NOM has been proposed. Physical access of competing compounds was restrained through manipulation of the porous structure of TiO_2 photocatalysts. An advanced templating method was employed to create a porous structure across TiO_2 nanoparticles. In this

study Ibuprofen as a target contaminant was decomposed in the presence of humic acid as competing NOM. Porous particles demonstrated significant improvement in selective decomposition of ibuprofen in the presence of humic acid as competing species. In the second phase of the study, a comprehensive study was conducted through changing the porous structure and size of co-existing organics in competing and non-competing conditions. The photocatalytic results, in correlation with material characterization demonstrated beneficial role of the controlled porous structure on adsorption followed by decomposition of organic species onto TiO_2 photocatalysts.

TABLE OF CONTENTS

LIST OF ILLUSTRATIONS

Figure Page

LIST OF TABLES

CHAPTER 1

INTRODUCTION

1.1 Advanced Oxidation Technologies

During past decades a substantial amount of synthetic organic compounds (SOCs) have been synthesized and discharged in environment. Persistency of SOCs to natural decomposition and their global distribution have generated considerable concerns in environmental sectors [1-2]. Studies demonstrated that conventional biological and physical treatment approaches suffer from efficient removal of most of these chemicals due to their persistency and their molecular size [3]. Among developing approaches, advanced oxidation technologies (AOTs) are gaining tremendous attention for treatment and remediation purposes because of their strength in decomposition of virtually all kind of organic contaminants [4-5]. AOTs are chemical procedures for generation of extremely oxidizing agents such as hydroxyl radicals (HRs) and sulfate radicals (SRs). The generated radicals can directly attack the organics bonds resulting in their breakdown and decomposition. Some of the generated radicals participate in propagation reaction resulting in production of oxidizing intermediates which can also attack the organics. It has been shown if sufficient time and chemical is given to reaction, organics undergo the complete mineralization [6]. The result of mineralization reaction is CO_2, H_2O, and other simple inorganic species (e.g., Cl^-, NO_3^- and SO_4^{2-}) which are totally harmless species for discharge to environment. Figure 1.1, demonstrates general scheme and concept of AOTs. Decomposition cycle is comprised of a series of chain reactions which are initiated with radical generation. Due to fast reaction rate of radicals and organic compounds, rate of radical generation governs the total kinetic of decomposition reactions.

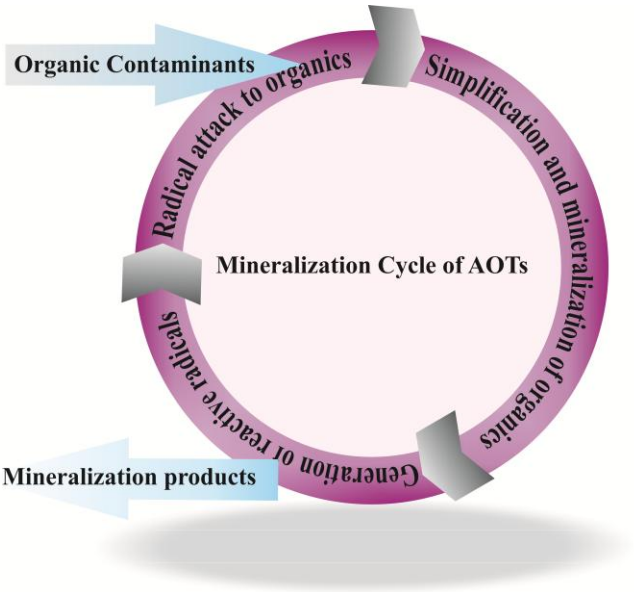

Figure 1.1 General Working Mechanisms of AOTs for Mineralization of Organic Contaminants

Attack of radicals to organics usually takes place in a multi-step reaction which can be breakdown to the following steps: i) generation of reactive radicals, ii) radical attack on organic molecules and formation of carbon-centered radicals in the organic molecules, iii) addition of oxygen and transformation of carbon-centered radicals to peroxyl radicals, and iv) breakdown of peroxyl radicals to simpler organic molecules [7]. Repetition of this cycle contributes to the breakdown and eventually mineralization of the organic molecular structure. This cycle is effective for almost any type of organics regardless of their molecular stability. These unique properties of AOTs make them a viable alternative treatment process for air stripping, GAC adsorption and resin adsorption. Unlike adsorption units which employ phase transfer process for treatment of water, AOTs destruct organic contaminants. Destruction of toxic organics eliminates concerns about waste disposal and regeneration of adsorption media.

It is also notable although attack of hydroxyl radicals and sulfate radicals to organics contributes to production of other intermediate radicals, AOTs are mostly related to direct reaction of hydroxyl and sulfate radicals with organics, since intermediate radicals suffer from enough

oxidizing power and usually lower reaction kinetic [8]. Hydroxyl radicals have a great reaction rate of 10^6-10^9 $M^{-1}.S^{-1}$ for most of organics, which is 10^6-10^9 times faster than hydrogen peroxide and ozone activity [9]. The highly oxidizing power of HRs also provides higher degree of decomposition which is not achievable through conventional oxidation processes. Table 1.1 shows relative oxidation power of HRs and most common oxidants.

Table 1.1 Relative Oxidation Power of Oxidants (Chlorine as Reference) [10-11]

Oxidizing Species	Oxidation Potential (Volts)	Relative Oxidation Power
Hydroxyl Radical	2.80	2.05
Activated Persulfate	2.60	1.88
Ozone	2.07	1.52
Persulfate	2.01	1.46
Hydrogen Peroxide	1.77	1.30
Perhydroxyl Radical	1.70	1.25
Permanganate	1.69	1.24
Chlorine	1.38	1.00
Oxygen	1.20	0.90

Great oxidation potential of HRs suits its application for extremely stable contaminants such as halogenated hydrocarbons (Trichloroethane, Trichloroethylene, Vinyl Chloride and …) as well as aromatic compounds (Benzene, Toluene, Ethylbenzene, Xylene) [9]. Various photochemical and non-photochemical pathways can be used for HRs production. Typically in non-photochemical pathways, a combination of common oxidants is used for radical generation.

Table 1.2 List of Typical AOT Systems [12]

Non-photochemical	Photochemical
O_3/H_2O_2	O_3/UV
O_3/OH	H_2O_2/UV
O_3 /GAC	H_2O_2/Fe_2+ (photo-Fenton)
O_3/US	O3/H2O2/UV
Fe_2+/H_2O_2 (Fenton system)	UV/TiO_2
electro-Fenton	H_2O_2/TiO_2/UV
ultrasound (US)	O_2/TiO_2/UV
H_2O_2/US	UV/US
O_3/CAT	
electron beam irradiation	

Typically in non-photochemical pathways, combinations of common oxidants are used for radical generation. While in photochemical approaches source of light, especially UV initiates and accelerates the rate of HR formation. Among previously established technologies Fenton's reagent have been extensively studied and used. However a concern about release of iron ions in effluent has a drawback effect of its widespread applications [13]. Also all the non-photochemical approaches require constant chemical loading. Recently photochemical approaches such as heterogeneous TiO_2 photocatalysts have been center of research in the field of AOTs.

1.2. Photocatalytic Materials and TiO_2-UV System

Photocatalysts are material with capability to use photon energy for initiation of chemical reactions. Heterogeneous photocatalysts are mostly semiconducting materials such as TiO_2, ZnO, ZrO_2, CeO_2, SnO_2, Fe_2O_3, $SbrO_4$ which can use photon energy for electron/hole generation among semiconducting material, TiO_2, ZnO, Fe_2O_3 have gained more attention for environmental application due to their low cost and green properties. . Zinc oxide (ZnO) can utilize visible-light although it has a wide band-gap of 3.3 eV. However solubility of ZnO in water has a drawback effect on its full-scale application due to health concerns about presence of Zn ions in water [14, 17]. Nanostructured α- Fe2O3 have been recently considered for water splitting reaction due to its low cost and chemical stability. Fe_2O_3 exhibit a direct band gap of 3.3 eV (375 nm), and indirect band gap of 2.06 eV which can utilize sunlight for activation [18]. However short excitation lifetime and poor charge carrier mobility of Fe_2O_3 limits their HRs generation yield and consequently their application [18]. Research efforts in photocatalytic water splitting have been significantly expanded after discovery of photocatalytic properties of crystalline TiO_2. TiO_2 photocatalysts utilize light energy as deriving force and atmospheric oxygen for HRs production which eliminates the need of chemical addition. They are also relatively cheap and exhibits high photo-chemical corrosive resistance [19-20]. When enough photon energy is absorbed by TiO_2 photocatalysts, the photon energy promotes an electron (e-) from valance band to conduction band, resulting in formation of hole (h+) in valance band, as shown in figure 1.2 .The minimum energy required for excitement of electron between two bands is 3.2 eV, which corresponds to absorption of 386 nm wavelength light. i.e. any photon with wavelength of 386 nm and smaller is capable of photo-excitement of TiO_2 material which lies in the UV range [20]. Most of the generated electron/hole pairs recombine after generation resulting in useless heat production. Recombination is undesired pathway of consumption of electron/holes which decreases HRs yield. Some of the generated holes migrate to the surface of TiO_2 photocatalysts and react with adsorbed species such as hydroxyl ion resulting in

generation of hydroxyl radicals ($OH^{\bullet}$). On the other hand, generated electrons can react with electron acceptors such as O_2 and produce oxide radical anions $O_2^{-\bullet}$ as shown in figure 1.2.

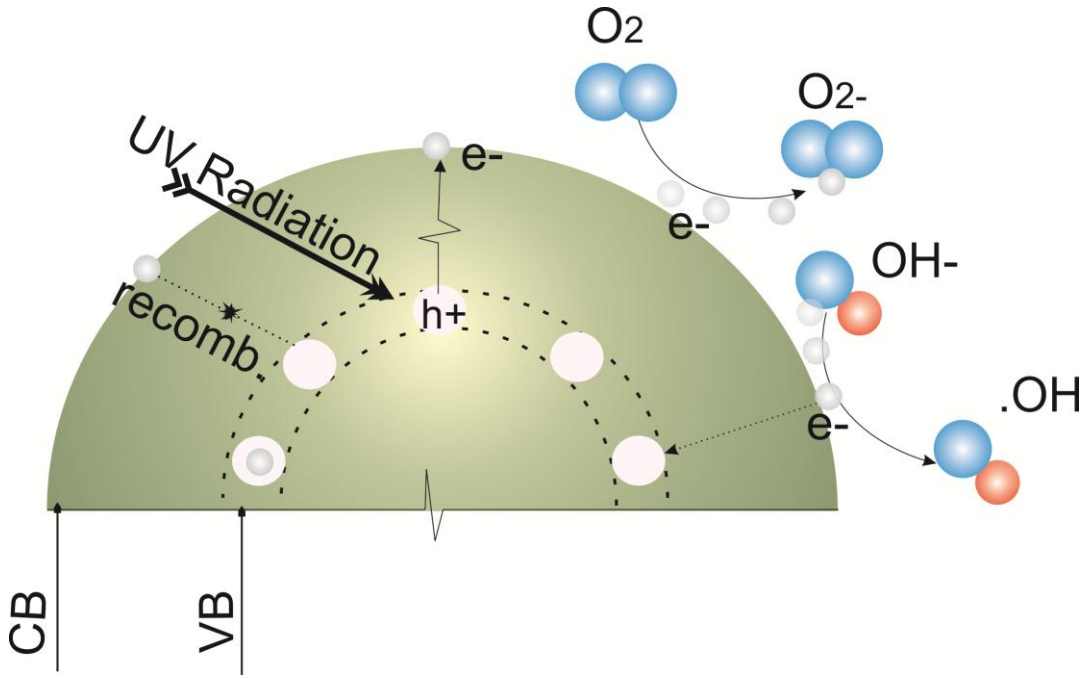

Figure 1.2 Illustration of Photocatalytic Generation of Reactive Radical Species in TiO_2-UV System. The Steps includes: Light Irradiation to TiO_2 Surface Followed by Electron Excitation from the Valance Band (VB) to the Conduction Band (CB), and Generation of Electrons (e-) and Holes (h+), Recombination of the Electrons and Holes, and Formation of Reactive Radicals by Redox Reactions on TiO_2 Surface

As illustrated in Figure 1.2, generation of oxidizing species requires reaction of generated holes and electrons with adsorbed species. Pre-adsorption of species is a requirement for accelerating redox reactions due to short life-time of electron/hole pairs. Equations 1.1 through 1.3 express the reaction pathway of HRs generation [9]:

$$TiO_2 + UV \longrightarrow e^- + h^+ \qquad \text{eq. 1.1}$$

$e^- + O2 \longrightarrow O_2^{-\bullet}$ eq. 1.2

$OH^-(ad) + h^+ \longrightarrow OH^{\bullet}(ad)$ eq. 1.3

TiO_2 exist in three major morphological shapes. Amorphous TiO_2 doesn't exhibit significant photocatalytic activity due to its defect structure. Defect structure inhibits mobility of generated electron/holes to the surface of catalysts [21]; As a result redox reaction cannot be initiated. Crystalline TiO_2, anatase and rutile show much more photocatalytic activity. Rutile TiO_2 has a lower band gap (3.0 eV) compared to anatase (3.2 eV) which facilitates electron excitement however due to fast recombination of electron/holes it exhibits a lower Photocatalytic activity compared to anatase [22]. TiO_2-UV system have shown to be effective for decomposition of persistent organics such as dyes [23], benzene derivatives [24-25], PCB's [26], pesticides [27-31] , explosives [32], detergents [33], cyanobacterial toxins [34] through photocatalytic decomposition. Semiconducting material also can be used for transformation of inorganic pollutants to non-toxic or less toxic species. cyanides ([35-36] , thiocyanates [37], cyanates [38], bromates [39], arsenic(III) and chromium(VI) has been observed during the redox reactions using semiconductors [40-43].

1.2.1 Challenges and Limitations of TiO_2-UV System

Hydroxyl radicals are strong oxidants which non-selectively attack and decompose any present organic in water [44-45]. Non-selectivity of HRs implies its applicability for any combination of organic contaminants. However a deeper insight into system reveals the problems associated with non-selectivity. In water resources we are usually dealing with a high concentration of naturally organic matters, (i.e. organic interferents, microorganisms and humic substances) along with trace level water contaminants. Due to non-selective nature of HRs. a great portion of generated HRs are consumed through undesirable reaction with non-toxic, competing organics which results in significant decline in decomposition rate of target

contaminants [46-47]. As a result greater energy input and reaction time is required for effective removal of toxic organics which increases treatment costs. To overcome this challenge some researchers proposed approaches to enhance selectivity.

1.2.2 Conventional Approaches for Enhancing Selectivity

To Increase selectivity of photocatalytic reaction toward some specific compounds many researchers have considered physical and chemical modifications of TiO_2 structure. However the success in this field is partial and in most cases very specific, i.e. these strategies are only applicable for a particular compound. It has also been demonstrated that changing reaction condition can be useful for an specific class of chemicals.

1.2.2.1 Changing Reaction Conditions

One of the simplest ways to change the preferential adsorption of species can be achieved by changing reaction parameters such as temperature, residence time and pH. Muradov et al. [48] reported slightly different reaction rate for nitroglycerine, ethanol and acetone at elevated temperatures (80°C) compared to lower temperature (20°C). The phenomenon can be attributed to thermo-catalytic decomposition of species along with their photocatalytic degradation. Also torture affects adsorpticity of compounds. Keeping in mind that TiO_2 has isoelectric point of pH 6- pH 7.5 [49-51], changing pH below and above this range can result in preferential adsorption. This implies pH values higher than 7.5 can enhance adsorption of positively charged compounds. On the other hand pH values less than 6 are favorable for adsorption negatively charged contaminants [52-53].

1.2.2.2 Chemical Modification of TiO_2

Chemical modifications of TiO2 with introduction of other substances or doping with other elements can aim the preferential adsorption and/or reaction pathway. It has been demonstrated that doping TiO_2 with nobel metals such as Pd and Pt can control the cathodic process of oxygen reduction. This approach is useful for decomposition of contaminants that have a different pathway for photocatalytic degradation. For example doping can enhance

reaction kinetic with ethanol and methanol while decreasing reaction kinetic of chloroform, trichloroethylene [54].Other approaches concern changing structure of TiO_2 photocatalysts with introduction of substances which has affinity toward target contaminants. Over-coating TiO_2 surface with a hydrophobic compound such as n-octyltriethoxysilane have shown to be effective in adsorption of 4-nonylphenol in the presence of concentrated phenol [55]. However decomposition of over-coated layer over time. Also an inert adsorption site with selective properties can be implemented in the vicinity of TiO_2 photocatalysts. So called inorganic adsorb-and-shuttle is based on the adsorption of the contaminants on inorganic domains located at the vicinity of the photocatalyst, followed by their surface diffusion from the inert adsorptive sites to the photocatalytic surface [49]. However there is a possibility of diffusion to places other than photocatalytic surface which can reduce the effectively of this strategy.

1.2.2.3 Physical Modification of TiO_2

Physical modifications are approaches based on separation of species based on their molecular size. In this class of modifications, a secondary meso-porous layer such as SiO_2 with well-defined porous structure can control the mass transport of large size compounds onto active surface of TiO_2 photocatalysts. The small pores of SiO_2 layer implies restraining physical access of huge NOM while providing diffusibility of small size target contaminants. Similarly imcorporation of TiO_2 into sheet silicates of clay can induces same separation mechanism for the case that we are dealing with a mixture of organic compounds with significant size difference [49]. However current physical approaches necessitates incorporation of a secondary material which can imply complex synthesize route along with greater cost. Also encapsulating TiO_2 with a non-reactive material can raise the concern about the mass transfer limitations.

CHAPTER 2

MANIPULATION OF POROUS STRUCTURE OF TiO_2 TO ENHANCE SELECTIVE DECOMPOSITION OF IBUPROFEN

INTRODUCTION

In this study a novel size-exclusion approach for enhancing selective decomposition of ibuprofen (IBP) was proposed. This approach is based on control of mass transfer of competing organic compounds through suppressing their physical access to active surface of TiO_2 photocatalysts. Interestingly this task was done through modification of pure titania material instead of incorporating a secondary porous material. An advanced templating method was employed to manipulate the porous structure of TiO_2 nanoparticles. Porous TiO_2 nanoparticles were synthesized through modification of sol-gel method with introduction of organic amphiphilic molecules (surfactants) during sol preparation. Large size humic acids (HA) and small size IBP target contaminants were used in competing and non-competing reaction conditions. Photocatalytic behavior of porous TiO_2 was investigated in competing and non-competing conditions and was compared to photocatalytic behavior of non-porous TiO_2 nanoparticles. The photocatalytic results suggested the efficiency of proposed approach for selective decomposition in competing conditions.

2.1. Proposed Approach to Enhance Selectivity

The short life-time of HRs necessitates pre-adsorption of organic species on the TiO_2 surface for oxidation reactions [56]. As a result preferential adsorption of organic species is a key for enhanced selectivity. In the water treatment train we are mostly dealing with trace level water contaminants such as endocrine disrupting compounds and pharmaceutical

and personal care products along with greater concentration of naturally organic matters. It is notable molecular size of most of contaminants is usually significantly smaller than naturally organic matter (NOM) which implies their separation based on size [57-58]. In this study we propose engineered TiO_2 nanoparticles with strategically designed porous structure. As shown in figure 1.3 mesoporous structure of TiO_2 photocatalysts are designed so that only target contaminants are allowed to enter and be adsorbed on active surface of TiO_2 nanoparticles.

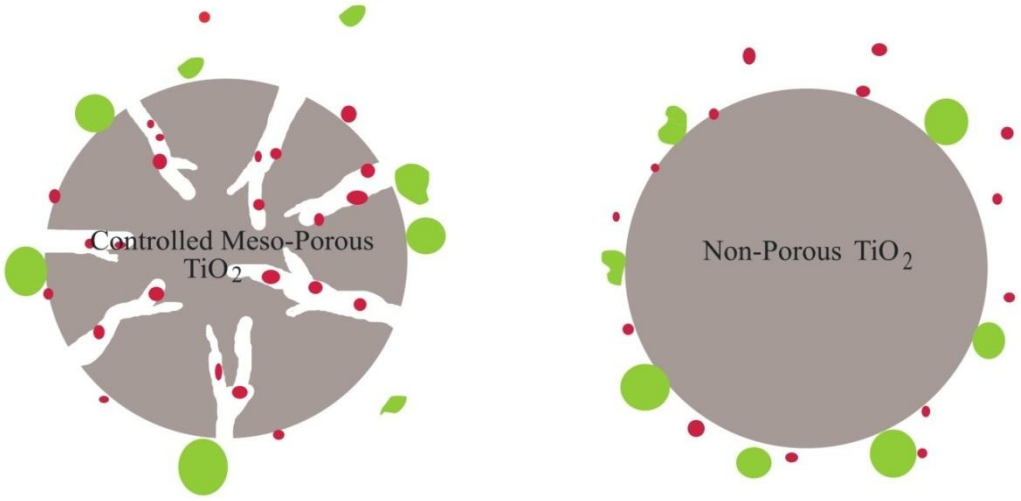

Figure 2.1 Selectivity Enhancements on an Engineered TiO_2 Nanoparticle with Controlled Mesoporous Structure. Due to the Small Throat Size of the Porous Structure (Which Provides Most of Adsorption Sites), NOM is Excluded from Adsorption into the Porous Structure, while Small Target Chemicals can Diffuse into TiO_2 Network for Decomposition

Compared to non-porous TiO_2 which has no preference for adsorption of species, the proposed nanoparticles is capable of providing adsorption sites in a zone that is only accessible for small target contaminants. Implementation of this strategy requires precise control on structural properties of synthesized TiO_2 nanoparticles. Pore size and throat size of network should be altered in a range close to molecular size of target compound to investigate the efficiency of proposed approach. Due to multidisciplinary nature of adsorption which is comprised from fluid

motions, diffusion and competing adsorption, optimum pore throat size cannot be predicted since there is a tradeoff between selectivity and mass transfer.

2.2 Methodology: Sol-Gel Synthesize of Porous TiO_2 Photocatalysts

Sol-gel is a popular method for fabrication of inorganic with controlled structural decomposition. These methods consist of wet-chemistry based procedures for synthesize of solid inorganic materials from their liquid precursor without melting at elevated temperatures. Process usually consists of four major steps: I) preparation of sol containing inorganic material through hydrolysis and condensation reaction of inorganic precursor ii) evaporation of the solvent and other volatile compounds which results in solidification of the gel iii) drying with controlled rate iv) Thermal treatment [59].

Sol-gel methods have major advantages compared to other deposition methods including: i) diversity in precursor selection ii) dopant and other additives can be easily incorporated during sol preparation iii) the properties of synthesized inorganic can be precisely tuned by changing concentration and other synthesize parameters [59].

2.2.1 Self-assembly of Surfactants and Formation of Micelles

Surfactants are organic molecules composed of a hydrophilic polar head and a non-polar or hydrophobic tail. This dual nature of surfactants tends to form unique structures of surfactant molecules based on thermodynamic principles. Among these unique properties their tendency to segregate their hydrophobic tail from water. So-called process of self-assembly results formation of cylindrical, spherical or plannar micelles above their critical micellar concentration (CMC) [60]. Solution conditions, concentration and surfactant functional group determine the shape and size of the formed micelle or vesicles. Van der Waals forces and hydrogen bonds hold the molecules in a cluster [61]. Common sol-gel methods for synthesize of TiO_2 photocatalysts are usually facing two major challenges. First, formation of amorphous TiO_2 which has a lower photocatalytic activity. Second, production of non-porous photocatalysts with limited adsorption surface area. In common sol-gel routes fast hydrolyze of highly reactive

alkoxide precursors results in unfavorable precipitation of amorphous particles with uncontrolled structure [62]. In this study to control hydrolysis and polycondensation reactions in a water-based, sol-gel method addition of organic additives, and coordination chemistry have been established. In-situ formation of water with a controlled rate is one of the proposed approaches for this sake. Also to generate a porous network across TiO_2 material, self-assembly agent was added to sol. Tween 80 with a concentration higher than its CMC was used as pore directing agent. The uniform micelles act like a template for TiO_2 network. During thermal treatment organic templates are pyrolyzed, leaving behind a hollow structure similar to micelle shape. In this study polyoxyethylene sorbitan monooleate (Tween 80) was used as templating agent. As shown in figure 2.2, Tween 80 with Lauric acid as hydrophobic group tends to form an inorganic network on self-organized organic molecules in the sol.

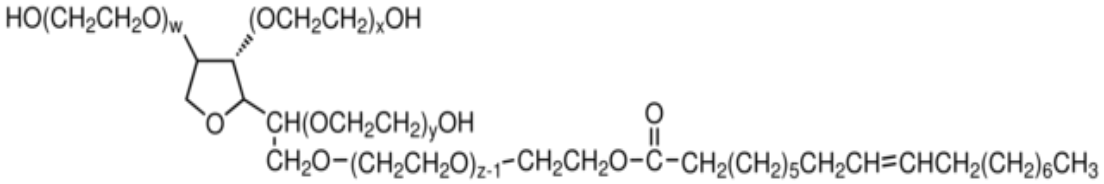

Figure 2.2 Amphiphilic Molecular Structure of Polyoxyethylene Sorbitan Monooleate (Tween 80)

2.2.2 Modified Sol-gel Process with Templates

Meso-porous TiO_2 particles were synthesized through addition of Tween 80 to sol during sol-gel synthesis. An appropriate amount of Tween 80 above its critical micellar concentration was vigorously dissolved in isopropyl alcohol. Great concentration of Tween contributes to self-assembly of micelles across the sol as depicted in figure 2.3 (i). Acetic acid was added into the solution for the esterification reaction with isopropanol. This reaction yields to in-situ generation of water molecules with a controlled rate. Then tetraisopropoxide was

added as titanium precursor. Reaction of TTIP and water molecules results in hydrolysis and condensation reactions figure 2.3 (ii).

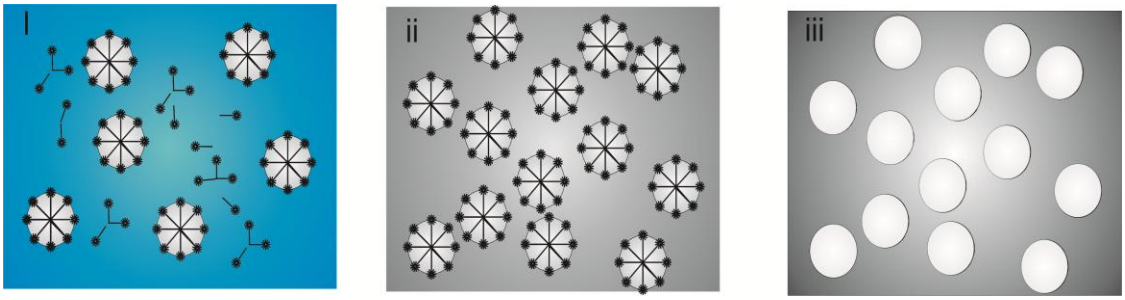

Figure 2.3 Synthesis Route for Synthesize of TiO_2 Matrix via a Sol-gel Method Employing Surfactant Self- assembly as a Pore Template: (i) Surfactant Self-assembly into Micelles in Water-rich Environment (ii) Titanium Alkoxide Precursor Hydrolyzation and Condensation to Form a TiO_2 Inorganic Network Around the Self-assembled Surfactant, and (iii) Porous TiO_2 Inorganic Network is Formed After Removal of the Organic Template by Thermal Treatment or Organic Extraction.

The amount of Tween80 was set to two times molar ratio compared to TTIP which implies templating role of added surfactant. Also a set of control particles were synthesized with similar procedure without addition of Tween 80. Fabricated gel was spread in a petri dish and held for 24 hours in room temperature for evaporation of extra solvent. Drying is a critical stage in sol-gel method since fast drying can result in defect structure across inorganic network due to evaporation pressure. Dried gel was later heat treated using a multi-segment programmable furnace. The thermal treatment at elevated temperature pyrolyzes organic templates leaving behind a hollow structure of TiO_2 as shown in figure 2.3 (iii). Also thermal treatment is beneficial in enhancing crystalline properties of TiO_2. Since anatase phase is known to have the best photocatalytic activity. The gel was calcinated at 500°C in a muffle furnace (Paragon, Sentry

2.0). The calcination time was set to 2 hours and slight ramp of 3 C°/min was applied to prevent defect structure.

Higher calcination temperature and longer calcination time can result in unwanted anatase to rutile phase transformation. Also high temperature ramp will create defect though TiO_2 matrix due to high pyrolysis pressure of organic templates. After calcination the TiO_2 material was naturally cooled down and grinded to obtain one set of meso-porous and one set of non-porous TiO_2 nanoparticles as shown in Figure 2.4.

Figure 2.4 Sample of Synthesized Porous TiO_2 Nanoparticle.

2.3 Selectivity of Meso-porous TiO_2 Nanoparticles

Aim of this part of study is to evaluate efficiency of proposed approach for enhanced selective adsorption and decomposition of target contaminant. Synthesized TiO_2 nanoparticles were used in two scenarios. In first scenario pure solution of ibuprofen was subjected to photocatalytic decomposition. Results of this experiment were later compared to competing condition. In competing condition HA was added to solution to as coexisting organics. Based on our hypothesis, in porous nanoparticles, most of the adsorption sites is located in the porous network of TiO_2 photocatalysts where there HA cannot penetrate due to their larger molecular size. Also different molecular sizes of HA were used in similar experiments to evaluate the effectiveness of size-exclusion mechanism.

2.3.1 *Physiochemical Properties of Ibuprofen*

Proposed TiO_2-UV aims to selectively decompose frequently found organic contaminants in water resources. Table 2.1 lists a number of common synthetic organic contaminants in water along with their molecular size. It is noticeable that molecular weight of most of these compounds is below 250 Da which implies the great size difference between NOM and organics to be removed. 2-[4-(2-methylpropyl) phenyl]propanoic acid (Ibuprofen) with molecular weight of 206 Da was selected for this study. Ibuprofen high solubility and low volatility contributes to its presence in aquatic environment. Physiochemical properties (i.e. high water solubility, low volatility) suggest a high mobility in the aquatic environment, and consequently, it is commonly detected PPCPs in the environment [64-65]. In a comprehensive study conducted by US-EPA on finished drinking water, revealed that among six most frequently reported active pharmaceutical ingredients (APIs), ibuprofen and its methyl ester metabolite are the only ingredients with frequently reported concentration of higher than 1 $\mu g.L^{-1}$. Beside direct adverse effect of APIs, their potential transformation during treatment process and formation disinfection byproducts (DBPs) that are unique to APIs generates an increasing health concern [66]. In this regard, oxidation processes should be applied with extensive

cautions, due to potential formation of DBPs and reaction intermediates with greater combined toxicity of parent APIs.

Table 2.1 Synthetic Organic Contaminants of Water [67]

Compound	Molecular Weight (Da)
Benzene	78
Bromobenzene	157
Bromodichloromethane	163
Bromoform	252
Bromomethane	95
Carbon Tetrachloride	154
Chloroethane	65
Chloroform	119
Dibromomethane	174
Ethylbenzene	106
Hexachlorobutadiene	261
Ibuprofen	206
Methyl t-butyl ether [MTBE]	88
Monochlorobenzene	113
Naphthalene	128
Styrene	104
Toluene	92
1,2,4-Trichlorobenzene	181
1,1,1-Trichloroethane	133
Vinyl Chloride	63
Xylene,	106

It has been demonstrated that 2-(4'-isobutyl-phenyl)ethanol and p-isobutyl acetophenone are two main intermediates of oxidation of ibuprofen. The yield of different oxidation products is depends on reaction conditions [68]. The molecular structure of ibuprofen has been illustrated in figure 2.5. ibuprofen is relatively hydrophobic with pKa of 4.43 [68].

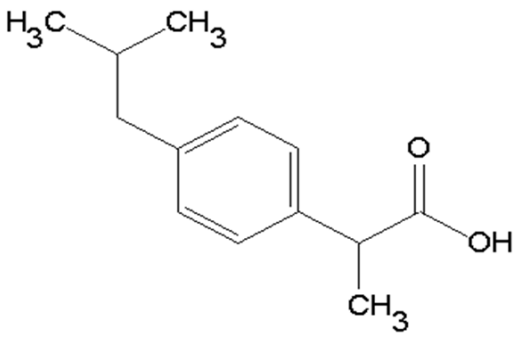

Figure 2.5 Structure of 2-[4-(2-methylpropyl) Phenyl]propanoic Acid (Ibuprofen)

2.*3.2 Physiochemical Properties of Competing Compounds*

Naturally organic matters and Humic substances are aboudant organic compounds in water resources. In this study, humic acid (HA) with large molecular size $C_{187}H_{186}O_{89}N_9S_1$; 4012 $g.mol^{-1}$, Aldrich) were used as competing organic compounds. Molecular size, solubility and pKa are of substantial parameters in adsorption behavior of substances. HA with hydrophobic properties similar to ibuprofen were used to minimize effect of surface chemistry on the adsoption process. The size of competing HA was intentionally selected in large range to induce the effect of size on the adsorption of different species.

2.4. Photocatalytic Behavior of Porous TiO_2 Photocatalysts

Photocatalytic experiments were employed to demonstrate the role of generated void structure in the selective behavior of catalysts. Two parallel set of experiments in competing and non-competing conditions were established for comparison. In each case reactor was

comprised of cylindrical cell, placed under two 15 W integrally filtered low pressure mercury UV tubes. Initial concentration of ibuprofen was adjusted to 12 mg (TOC).L^{-1}. In the batches containing HA similar concentration of 12 mg (TOC).L^{-1} was used. Figure 2.6 shows the configuration of UV irradiated reactors for competing and non-competing case.

Figure 2.6 Configuration of Photo-Reactors Equipped with UV Lamps

The TiO_2 nanoparticles were completely ground and pre-dispersed in water by sonication. The following experimental conditions were kept constant: initial volume of reaction solution = 0.1 l; initial pH = 7.0 ± 0.1 without buffer and stirring speed of 240 rpm. TiO_2 concentration was adjusted to 500 mg.lit^{-1} for all batches. Samples were kept in dark condition for 60 minutes prior to UV irradiation for adsorption of species into TiO_2 surface. Two 15 W low-

pressure mercury UV tubes (Spectronics) emitting 365 nm UV radiation were used at a light intensity of 3.5 $mW.cm^{-2}$.

Constant mixing was applied to increase mass transfer of species and their contact to the catalysts surface. However mass transfer occurs through different pathways which can affect the effectiveness of proposed approach.

2.4.1 Analytical Methods

The concentration of ibuprofen was monitored using a reverse phase high performance chromatography technique (HPLC, 1200 series, Agilent) equipped with ultraviolet (UV) detector. Two sets of standard solutions were used to generate calibration curves for different ranges of ibuprofen concentration. Dilutions of 0.2, 0.5, 1, 2 mg. L^{-1} with R^2 values of 0.9994 another dilution samples of 5, 10, 15, 20 mg. L^{-1} with R^2 values 0.9997 were employed to monitor ibuprofen concentration Figure 2.7 shows a sample of HPLC output and corresponding peak for ibuprofen at 4.45 minutes.

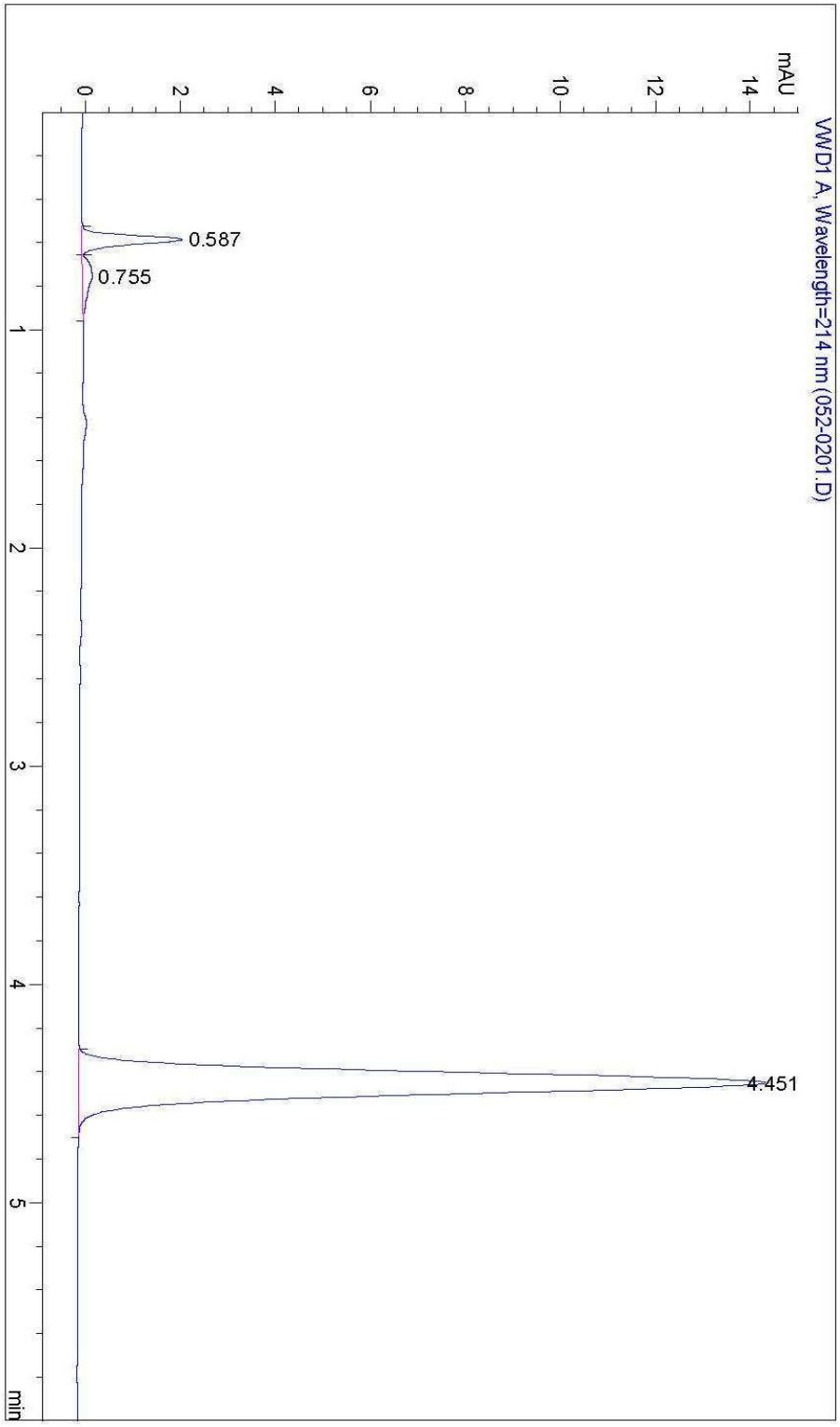

Figure 2.7 Example Chromatogram of Ibuprofen Peak Analyzed by HPLC

Samples were taken out at 15 minutes intervals and were filtered using syringe filters (0.45 µm) to remove TiO_2 nanoparticles . Preliminary studies demonstrated the adsorption of ibuprofen onto TiO_2 nanoparticles is very low, around 3 % of concentration which implies the change in concentration was only due to reaction and not due to adsorption onto porous TiO_2. A mixture of phosphoric acid buffer and acetonitrile was used as the mobile phase at buffer: ACN ratio of 50:50% v/v. The UV detector was set at a wavelength of 214 nm for detection of IBP with detention time of 4.45 minutes.

2.4.2 Decomposition of Target Compound

Figure 2.8 shows photocatalytic decomposition of ibuprofen using non-porous TiO_2 nanoparticles in both competing and non-competing scenario. As illustrated, pure ibuprofen solution has a relatively high decomposition rate which can be attributed to high surface area provided through excessive amount of photocatalyst during experiment.

On the other hand, in competing condition a great decline is observed in decomposition rate of target contaminant which can be correlated to parallel decomposition of HA along with ibuprofen.

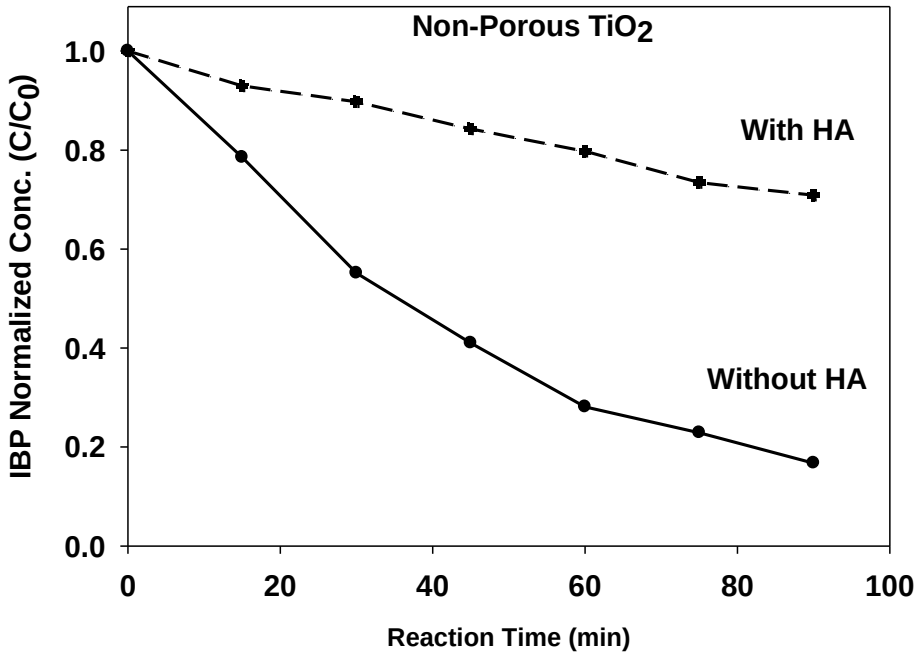

Figure 2.8 Photocatalytic Degradation of Ibuprofen Using Non-porous TiO_2 Nanoparticles

As proposed in scheme 1.3, most of the adsorption sites in non-porous particles are located on the surface of particles which has no selectivity for preferential adsorption of organics. In this case great portions of generated HRs on the surface of TiO_2 nanoparticle are consumed through undesirable decomposition of HA. Radical attack to the HA results in formation of organic intermediates which can further participate in decomposition reactions. Un-clustered intermediates have a greater specific surface area compared to parent HA which increases the chance of their participation in photocatalytic reaction. Figure 2.9 shows photocatalytic degradation of ibuprofen using different porous nanoparticles.

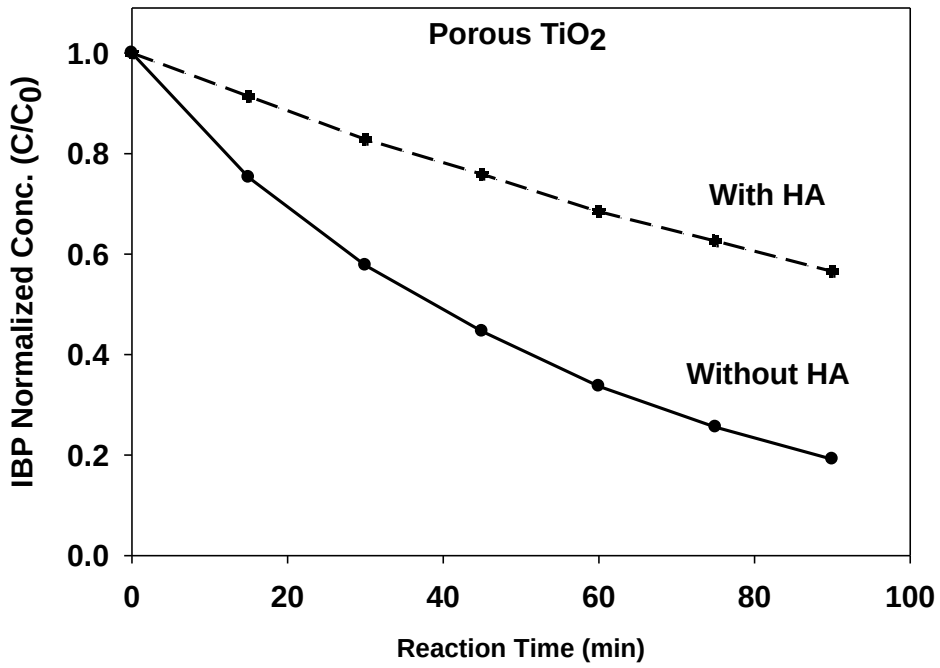

Figure 2.9 Photocatalytic Degradation of Ibuprofen Using Porous TiO_2 Nanoparticles

As shown in figure, porous particles represent more or less similar activity in non-competing scenario which can be attributed to high concentration of photocatalysts. The TiO_2 loading was intentionally chosen in saturation range of TiO_2 to eliminate the effect of enhanced surface area in the case of porous particles. In the used batches active surface area is not a limiting factor, implies that photocatalytic activity is only dependent on the physical access of species and porous structure of photocatalyst particles. In a lower concentration of TiO_2 loading porous catalysts with more than 10 times increased surface area have shown a significant improve in photocatalytic activity which is not aim of this study. Interestingly in competing condition the porous particles exhibit a significantly lower decline in photocatalytic activity. The proposed adsorption mechanism in scheme 1.3 suggests that in a well-defined porous structure of TiO_2,

larger size organic compound s (Large size HA) are effectively excluded from access to inter pore surface of particles which inhibit the parallel reaction of HA along with IBP.

CHAPTER 3

EFFECT OF PORE SIZE AND COMPETING ORGANICS ON SELECTIVE DECOMPOSITION OF IBP

INTRODUCTION

The aim of this part of study is to investigate the interaction of HA size and porosity on selective behavior of particles. First effect of surfactant on physiochemical properties and photocatalytic behavior of fabricated TiO_2 nanoparticles was examined. Different porous particles were synthesized through previously described method using different molar ratio of surfactant as pore directing agents. The synthesized particles were subjected to material characterization. TEM imaging techniques X-ray diffraction (XRD) analysis and porosimetry analysis were employed to understand the role of organic templates in porous structure of particles. Also different photocatalytic experiments were conducted using various porous TiO_2 photocatalysts. The results suggested that addition of surfactant up to some point can result in selectivity enhancement. The porous particles with the best selectivity were later used in different photocatalytic experiments. Photocatalytic results in correlation with material characterization, evidences the efficiency of proposed approach regarding size-exclusion mechanism.

3.1 Effect of Surfactant on Physiochemical Characteristics of TiO_2 Nanoparticles

3.1.1 Synthesize of Meso-porous Nanoparticles

Previously established route was used for synthesize with slight modification. Molar

ratio of surfactant was altered between 1 to 4 to generate particles with diverse porosity characteristics. Previous research works suggest that changing amount of surfactant above and below this range will create defect structure and very low porosity respectively [62].

3.1.2 Material Characterization

Crystallinity of the TiO_2 catalyst was examined through X-ray diffraction (XRD) analysis. In each scan 2θ was altered between 20 and 90 degree and step of 0.1degree. The XRD results exhibited distinct response peak at 25.6 degrees which corresponds to anatase crystalline phase [68]. As shown in figure 3.1, response peak at 25.6 degrees starts to decline along with increase in surfactant content which can be attributed to inhibiting effect of organic templates on Chrystal growth. Interestingly all the synthesized particles exhibit crystalline size close to 9 nm which is believed to be the optimum size for photocatalytic activity [69].

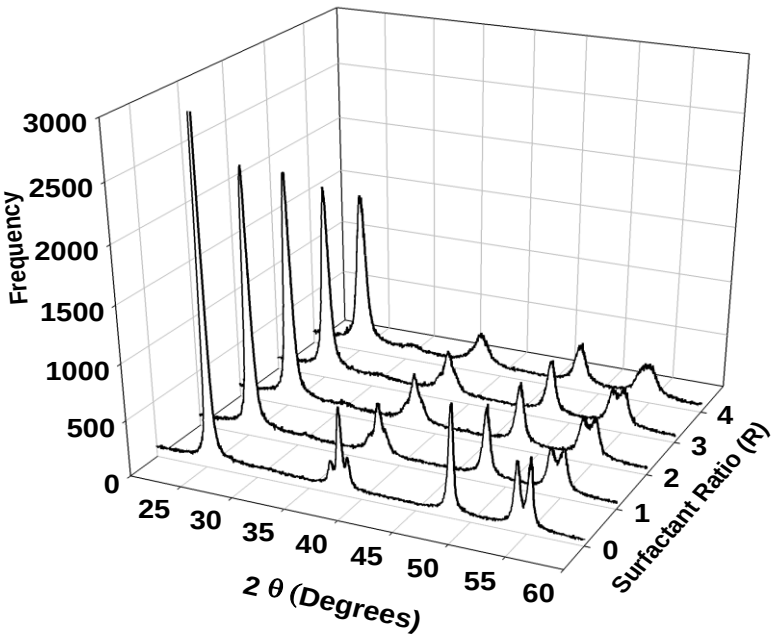

Figure 3.1 XRD Pattern of TiO_2 Material with Different Surfactant Ratios

Figure 3.2 shows HR-TEM images of different nano-crystalline anatase TiO_2 particles prepared though modified sol-gel method using Tween 80 (T80). As shown in figure 3.2 (a) control particles with no templating agents, does not show any distinct boundaries between particles. Also no regulated porous structure can be observed across TiO_2 material. Small random voids in the matrices can be attributed to organic impurities and colloidal particles in sol. On the other hand TiO_2 nanoparticles prepared with addition of pore directing agents in figures 3.2 (b) through Figure 3.2 (e) show almost spherical nanoparticles agglomerated into large clusters. Also a great portion of surface is covered with relatively well-defined porous structure.

The interconnected pore-network within TiO_2 material can facilitate diffusion of target organic to the network. As shown in figure 3.2 (f) images with higher magnification show randomly dispersed particles with explicit resolved lattice fringes which demonstrate high crystalline properties of TiO_2 material. It is also notable along with increase in surfactant content greater void structure forms across the TiO_2 network which evidences templating role of surfactant. It is also notable more interfacial defect structure was observed along with raise in concentration of surfactant. Higher chrystallinity of can be result of a combination of following pathways, i) atom by atom crystallization of anatase nanoparticles ii)direct aggregation of neighbor amorphous particles iii)solid-state aggregation of anatase particles.[70] presence of organics during heat treatment can also act as a crystalline inhibitor due to separation role of organics. As a result higher concentration of surfactant results in greater inhibition of crystal growth in the surrounding grain size, limiting the crystalline size which is in agreement with XRD results [71].

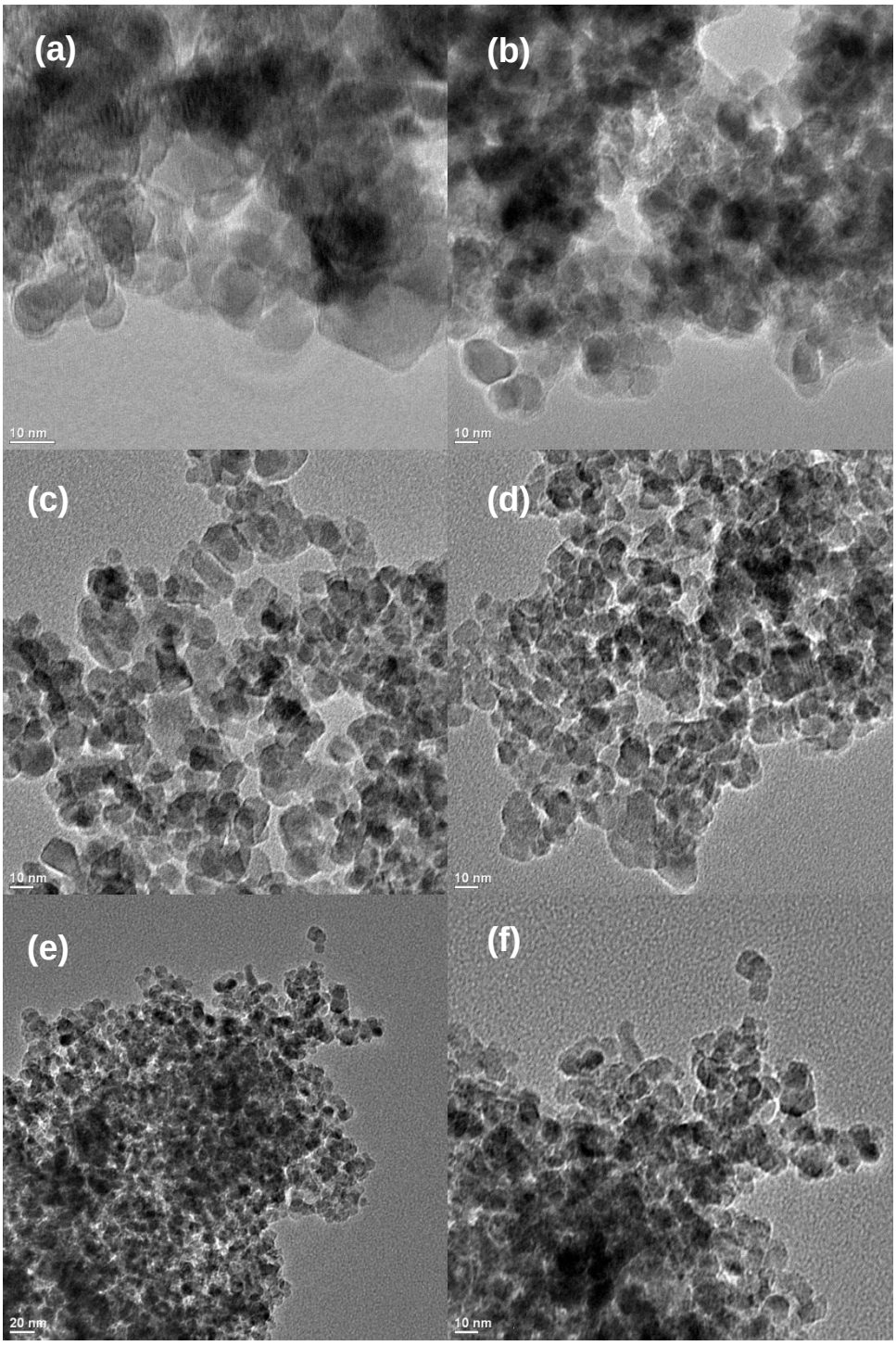

Figure 3.2 Figure 3.2 TEM Images of Crystalline TiO_2 Nanoparticles Prepared with (a) Control at R = 0. (b) T80 at R = 1. (c) T80 at R =2. (d) T80 at R =3. (e) T80 at R =4. (f) T80 at R =4 Higher Magnification.

Also elemental analysis of fabricated TiO_2 using Energy-dispersive X-Ray Spectroscopy (EDS) showed that both all control particles and porous particles exhibit similar response peaks around 0.5 and 4.5 KeV which correspond to excitation energy of O_2 and TiO_2 materials respectively. EDS results along with XRD patterns demonstrates similar elemental and crystalline properties of all synthesized particles.

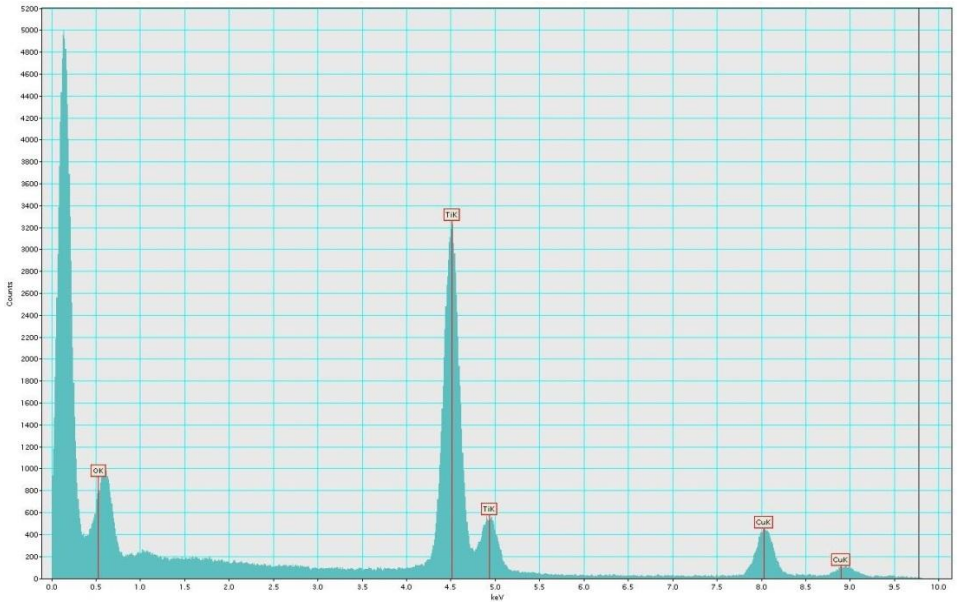

Figure 3.3 EDS Spectrum of Control TiO_2 nanoparticles

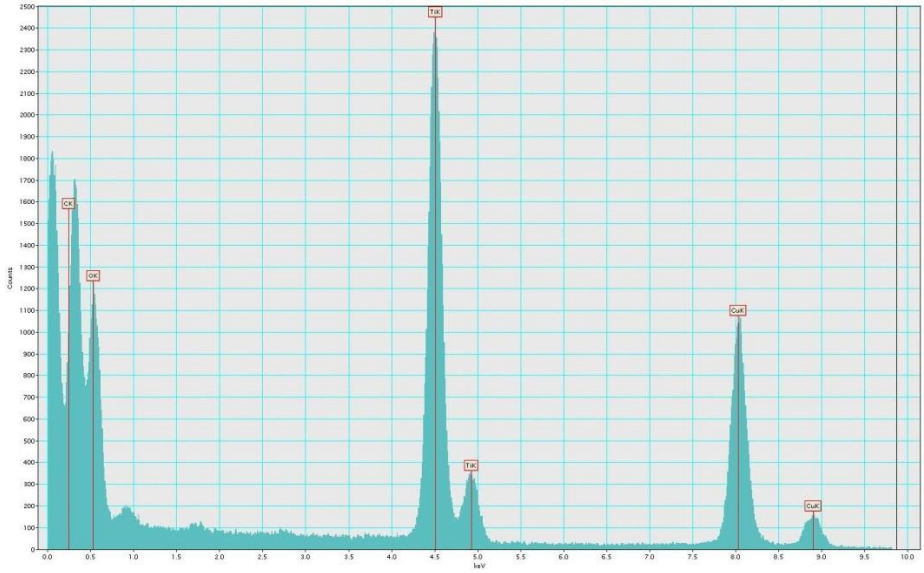

Figure 3.4 EDS Spectrum of Porous (P_1) TiO_2 nanoparticles

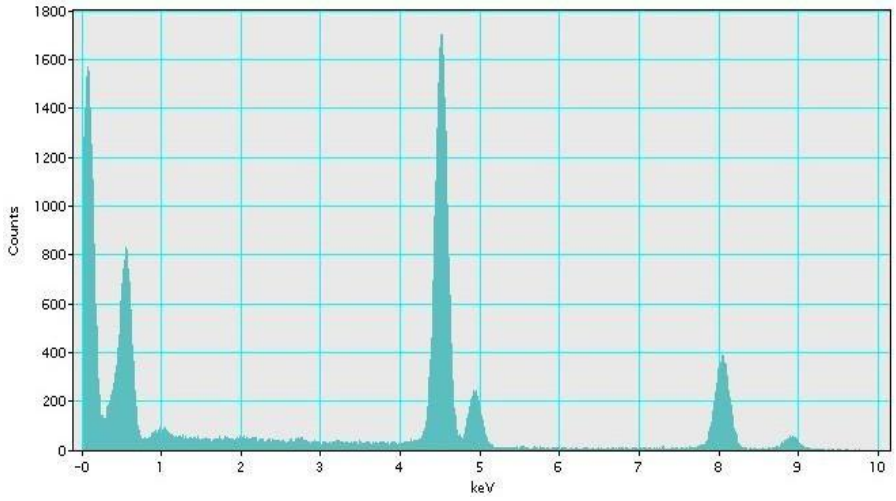

Figure 3.5 EDS Spectrum of Porous (P_2) TiO_2 nanoparticles

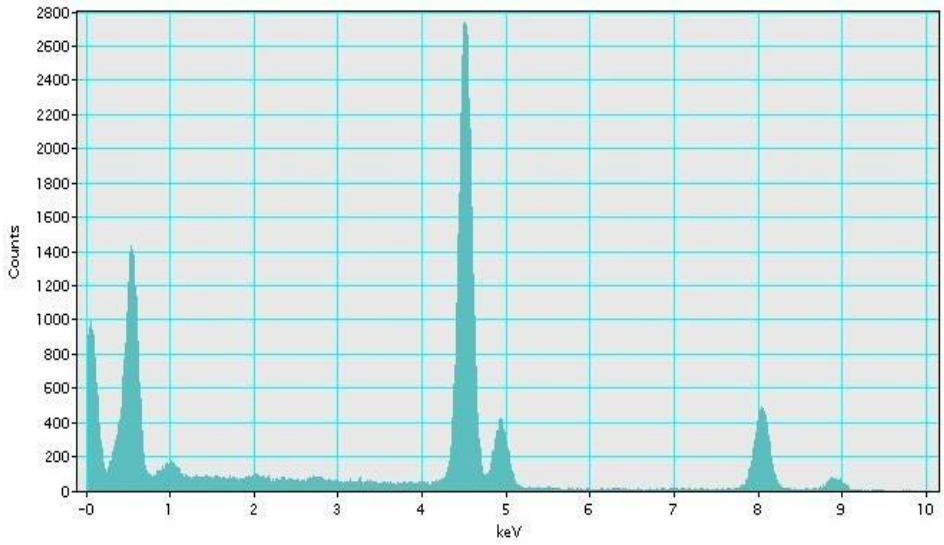

Figure 3.6 EDS Spectrum of Porous (P_3) TiO_2 nanoparticles

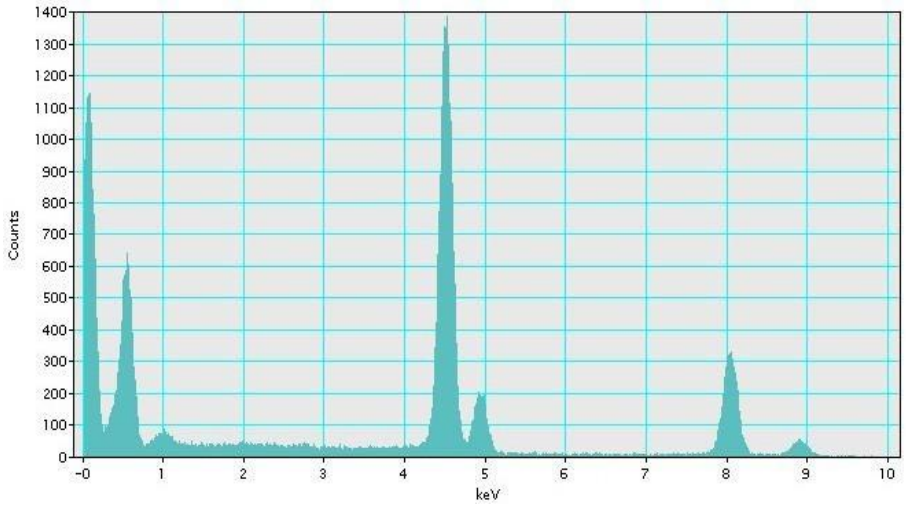

Figure 3.7 EDS Spectrum of Porous (P_4) TiO_2 nanoparticles

Porous structure of synthesized particles was examined through N_2 adsorption-desorption porosimetry analysis. As shown in figure 3.8 Compared to N_2 isotherm of control material which represents a negligible amount of pore volume around 5-8 nm, all porous material exhibit a significant void volume in the meso size range. Dissimilar hysteresis loop

observed for adsorption and desorption isotherms represents different throat size. The pore size distribution was also relatively narrow with a sharp peak in the range of 6-15 nm. Major structural properties of synthesized particles are summarized in table 3.1. The significant increase in BET surface area from 13.7 m^2g^{-1} to 110.9 m^2g^{-1} represents greater active surface area for better photocatalytic activity. Also greater surface of TiO_2 matrices with mostly inter-porous portion provides adsorption sites for selective decomposition of smaller compounds which is aim of this study.

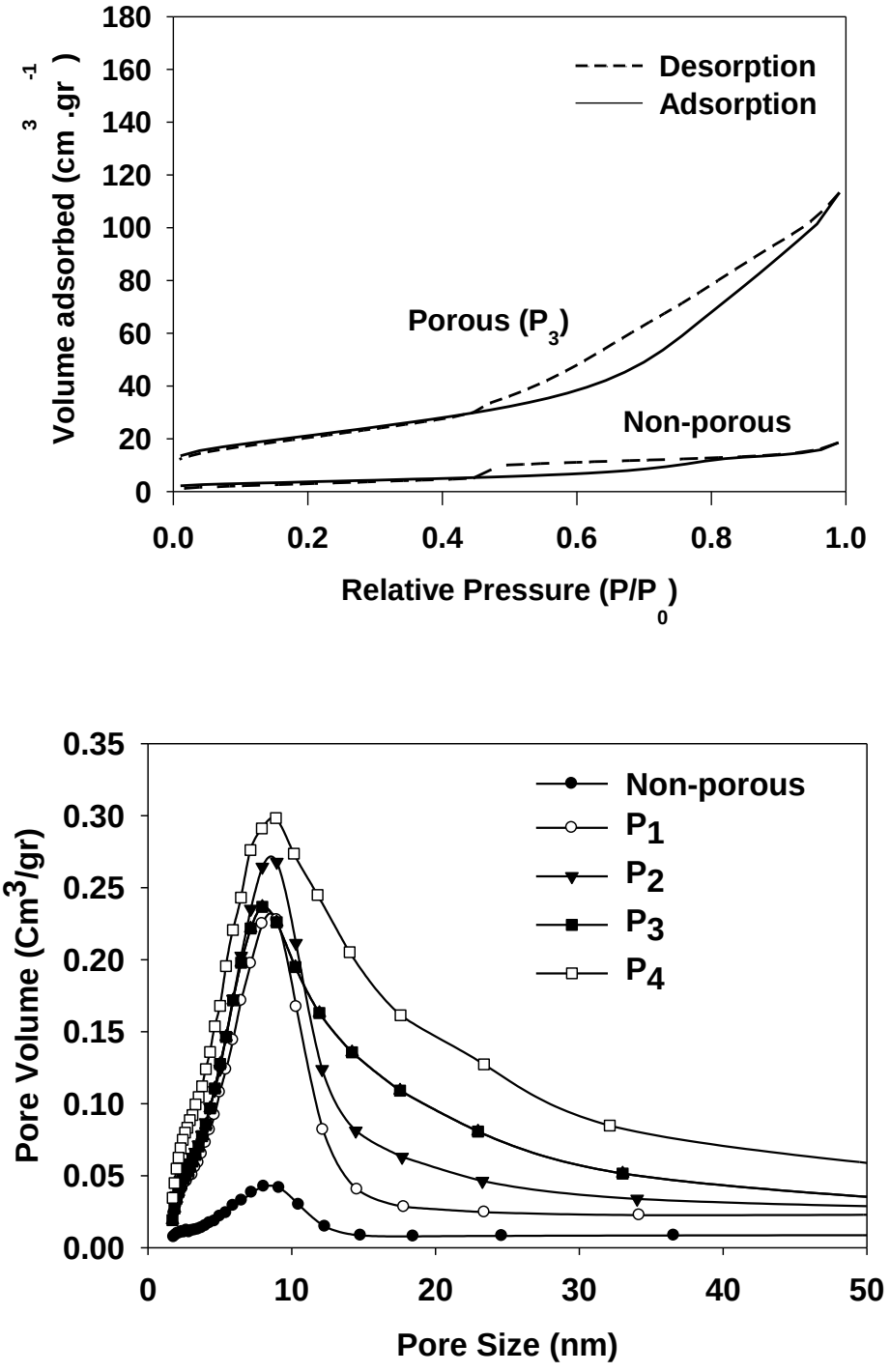

Figure 3.8 N_2 Adsorption/desorption Isotherms Pore Size Distribution of TiO_2 Material.

Table 3.1 Physiochemical Properties of TiO_2 Material

Parameter	Non-porous (R=0)	P1	P2	P3	P4
BET specific surface area [m^2g^{-1}]	13.7	61.42	76.4	76.5	110.9
Pore volume [cm^3g^{-1}]	0.028	0.123	0.159	0.175	0.253
Porosity [%]	10.6	34.2	40.2	42.5	51.7
BJH adsorption pore diameter [nm]	7.38	6.99	7.31	7.94	80.1
BJH desorption pore diameter [nm]	5.02	5.81	6.2	6.78	7.19
Crystal phase	Anatase	Anatase	Anatase	Anatase	Anatase

3.2 Effect of Porous Structure on Preferential Decomposition of IBP

3.2.1 Photocatalytic Decomposition of IBP

Conditions previously described in experimental section were kept constant in this part of study. Different TiO_2 nanoparticles with similar concentration of 500 $mg.L^{-1}$ were used in similar experiments. Figure 3.9 shows photocatalytic decomposition of ibuprofen using non-porous TiO_2 nanoparticles in competing and non-competing conditions . As established earlier pure ibuprofen solution has a relatively high decomposition rate compared to competing condition with ibuprofen.

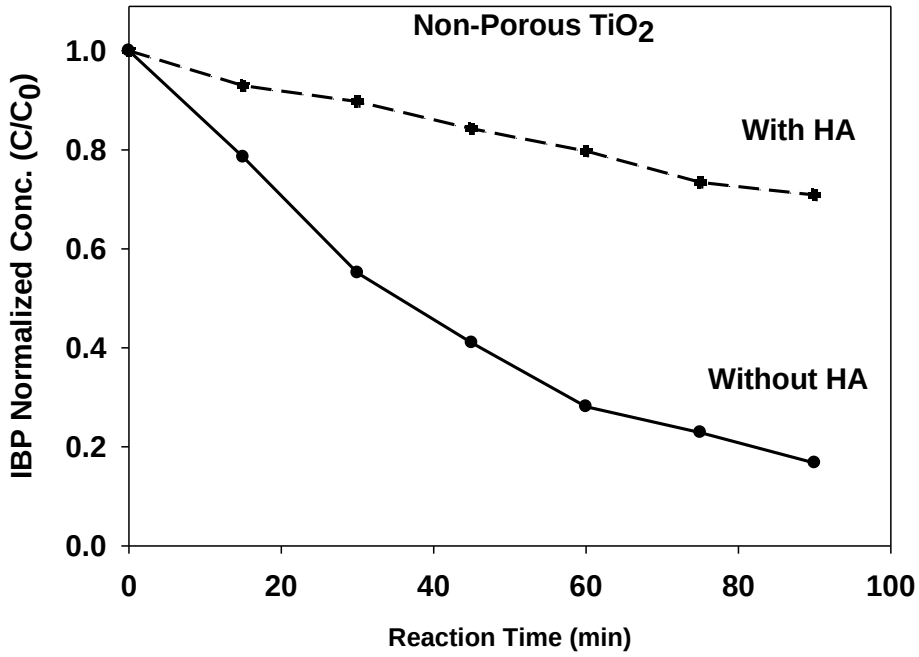

Figure 3.9 Photocatalytic Degradation of Ibuprofen Using Non-porous TiO_2 Nanoparticles

Similar conditions were applied to all setes of synthesized porour TiO_2 nanoparticles with various throat sizes. The larger fraction of HA was used in competing conditions and results were interpreted in respect to decomposition rate of IBP. Figure 3.10 -3.13 shows photocatalytic degradation of ibuprofen using different porous nanoparticles. P_1, represents less porous nanoparticles with surfactant content of 1 molar Tween 80 per mole of TiO_2 precursor. As shown in figures, all porous particles represent more or less similar activity in non-competing scenario which can be attributed to high concentration of photocatalysts. The TiO_2 loading was intentionally chosen in saturation range of TiO_2 to eliminate the

effect of enhanced surface area in the case of porous particles. In the used batches active surface area is not a limiting factor, implies that photocatalytic activity is only dependent on the physical access of species and porous structure of photocatalyst particles. In a lower concentration of TiO_2 loading porous catalysts with more than 10 times increased surface area have shown a significant improve in photocatalytic activity which is not aim of this study.

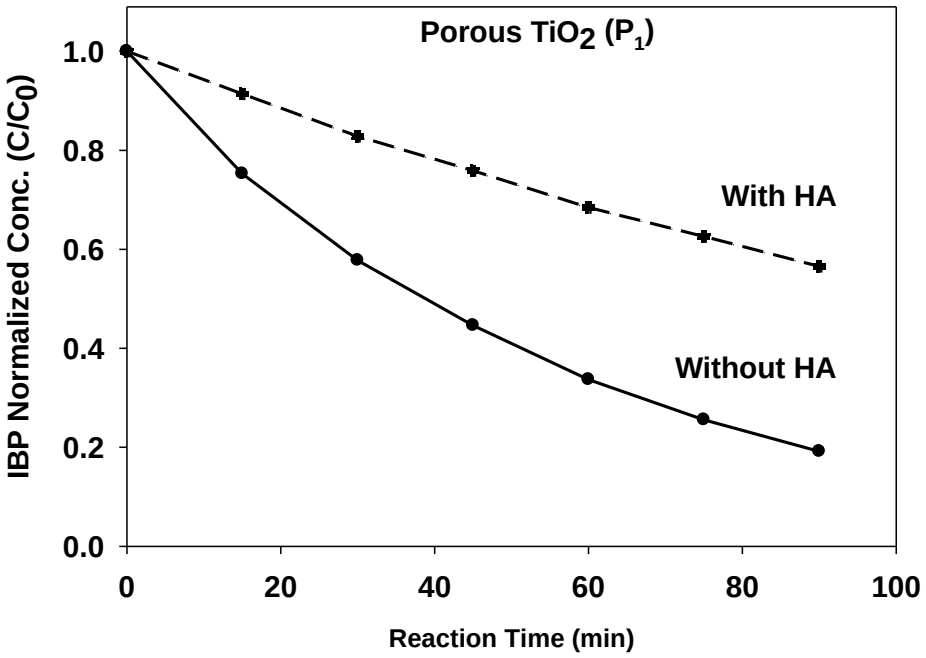

Figure 3.10 Photocatalytic Degradation of Ibuprofen Using Porous (P_1) TiO_2 Nanoparticles

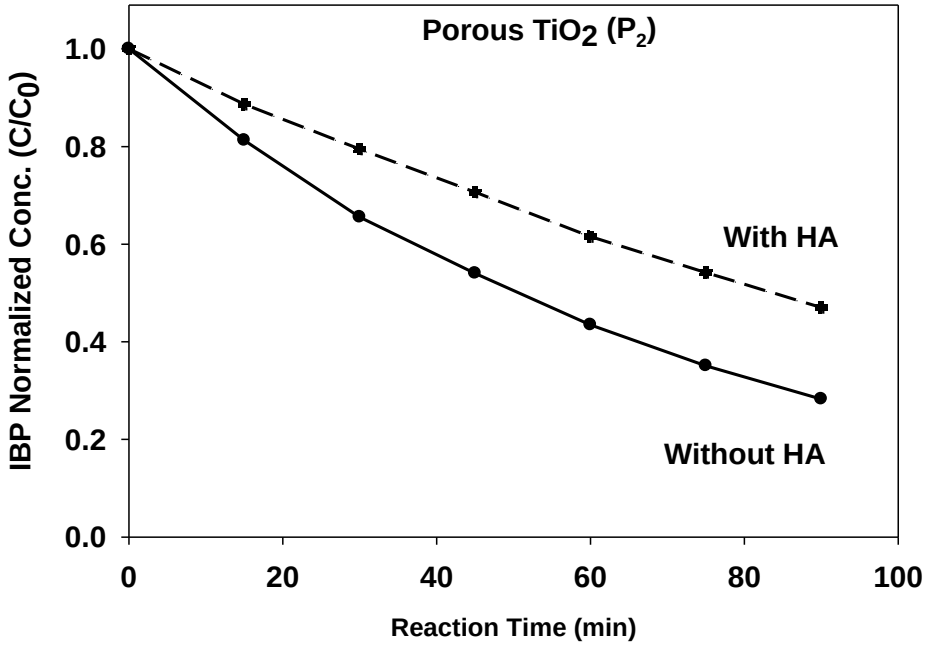

Figure 3.11 Photocatalytic Degradation of Ibuprofen Using Porous (P_2) TiO_2 Nanoparticles

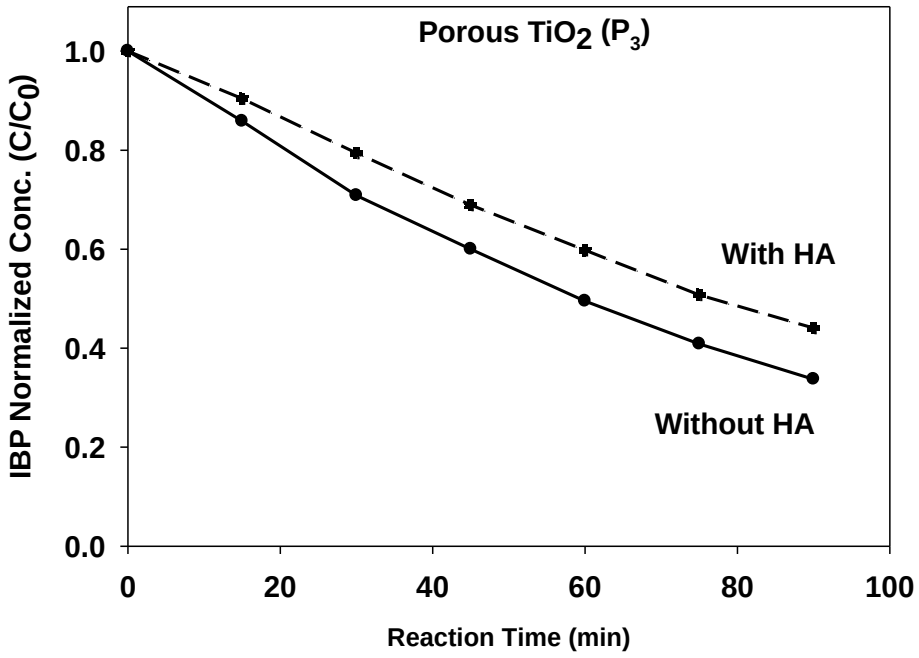

Figure 3.12 Photocatalytic Degradation of Ibuprofen Using Porous (P_3) TiO_2 Nanoparticles

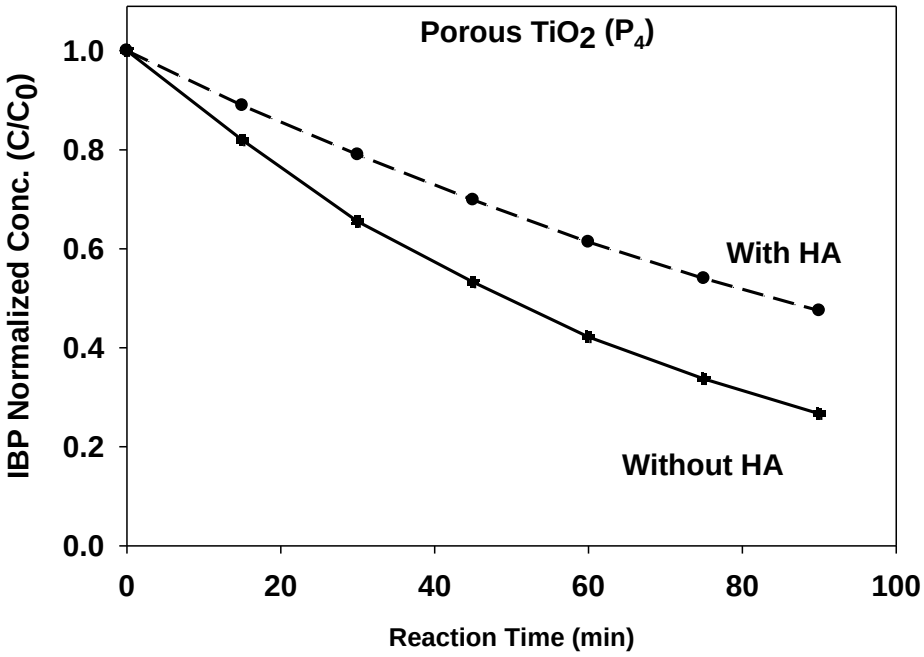

Figure 3.13 Photocatalytic Degradation of Ibuprofen Using Porous (P_4) TiO_2 Nanoparticles

As demonstrated in figures 3.10-3.13, all the porous particles exhibit lower decline in photocatalytic activity competing condition compared to non-porous particles. Result suggests that some of active sites in porous particles behave selective in decomposition of ibuprofen. It is notable the amount of selectivity recovery shows an increase along with raise in porosity and pore size. Results from porosimetry analysis also demonstrated higher inter pore surface area along with raise in surfactant content which implies more porous particles with most of their adsorption sites inside the TiO_2 network can better withstand the presence of competing HA. The enhanced activity also can be attributed to better diffusion of target contaminant in the case of larger throat size. As shown in figure 3.13 raising the surfactant content above 4 molar ratio of TTIP, yields in loss of selectivity compared to P_3. This phenomenon can be attributed to unfavorable decomposition of HA along with ibuprofen. Although larger pore size can facilitate the diffusion of ibuprofen, they cannot effectively restrain physical access of smaller portion of HA onto surface of TiO_2. TiO_2 nanoparticles with a considerable pore size above 20 nm have the possibility of entrance of smaller portion of HA into porous structure. They can also result in temporary clogging of pores.

3.2.2 Effect of Templating Agents on General Activity of TiO_2 Nanoparticles

As shown in Figures 3.9 through 3.13, despite greater BET surface area of porous TiO_2, the general activity of porous nanoparticles exhibit slight decline compared to control particles. It is notable that photo-excitation of TiO_2 material is dependent on effective adsorption of UV radiation on its surface. As illustrated in scheme, most of provided surface area is comprised of interconnected network of pores which are mostly located inside the particles. The limited accessibility of UV to aavailable surface implies partial activation inner surface area. Also In agreement with XRD patterns, change in crystalline properties of porous TiO_2 resulted from addition of surfactants can contribute to difference in reactivity of fabricated titania material. It has been established that, greater amount of surfactant can restrain crystal growth of titania material during calcination at high temperature. Smaller crystal can result in occurrence of so called phenomena of “blue shift” [72]. In this phenomenon along with decline in crystalline size, a greater amount of activation energy is required for generation of electron/hole pairs. Subsequently in spite of greater adsorption sites, lower amount of radicals are produced. Change in recombination rate of different porous titania, could affect the overall productivity of reactive radicals.

3.3 Effect of HA Size on Selective Decomposition of IBP

Porous particles with the best selectivity were later used reaction with different molecular sizes of HA as competing organics. The TOC concentration of HA was kept similar in all batches. The size distribution of the HA was examined through fraction experiment. Different fractions were later obtained through re-suspension of retained portion of HA in each filter step.

3.3.1 Fractionating the Humic Acid

Humic acid (HA) is a mixture of naturally organic macromolecules which is extensively found in water resources. They are important component of resource water quality since they can interfere with treatment processes and greatly effluent quality [73]. In aqueous form HA exhibit characteristics similar to polymeric structures [74]. It is believed that HA are supramolecular aggregate of very small molecules which are functionality held together by weaker hydrophobic interactions and hydrogen bonding [75-77]. Figure 3.14 shows model molecular structure of HA.

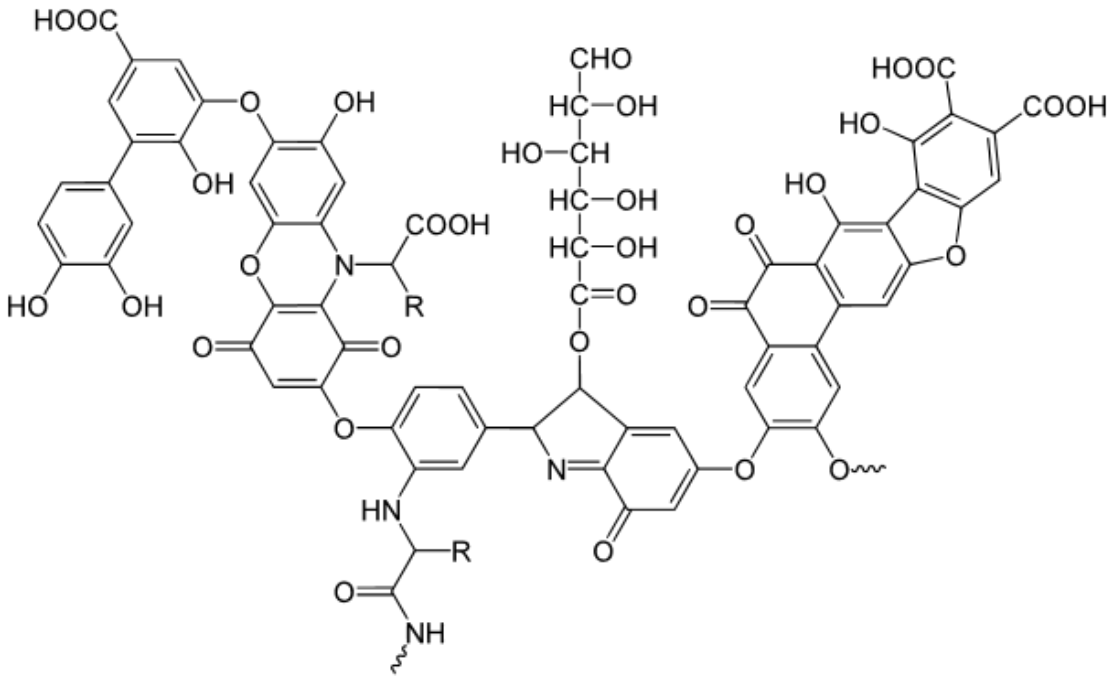

Figure 3.14 Model Structure of Humic Acid [78]

HA was selected as a competing compound during this study to illustrate real-case conditions. Also their hydrophobic properties and pKa similar to target compound, minimizes the effect of other adsorption parameters such as surface chemistry [79-81]. HA are organic substances with a wide molecular size and structure which makes it difficult to examine their effect on photocatalytic experiment. To obtain additional insight into size dependency of adsorption process HA size distribution was conducted through ultrafiltration method and each size fraction was used in similar photocatalytic experiments. Fractionation of HA was performed through a multistep ultrafiltration method. A stock solution of HA (from Sigma-Aldrich Company with initial TOC concentration of 200 $mg.lit^{-1}$ in DI water was prepared through vigorous mixing. Four different fraction size of HA were separated employing ultrafiltration cell (Amicon Model-8200 series) equipped with regenerated cellulose membrane discs. Each membrane disc was immersed into ethanol for three hours, rinsed with DI water and procedure was repeated three times to remove anti-drying agents from filtrate. Also cell was flushed with 100 ml of DI water before each experiment. During filtration constant stirring (240 rpm) was applied to membrane surface to prevent concentration polarization on the membrane surface. Concentration polarization results in formation of a boundary layer between active layer of membrane and solution which can contribute to

secondary membrane formation. Membrane discs with molecular weight cut off (MWCO) of 10 kDa, 30 kDa and 100 KDa (Millipore D 63.5 mm) were used to obtain four different molecular size of HA. Figure 3.15 demonstrates configuration of ultrafiltration cell.

Figure 3.15 Ultrafiltration of HA using Pressure Driven Filtration Unit Equipped with Magnetic Stirrer

Both stock solution and filtrate were analyzed using TOC analyzer (Shimadzo TOC-VCSH). Table 3.2 shows the relative TOC concentration of each fraction based on their TOC analysis.

Table 3.2 TOC Constitution and Percentage of Different Fractions of HA

Fraction	TOC (mg.L-1)	TOC Percentage (%)
F1 (>100 kDa)	25	12.5
F2 (30 kDa-100 kDa)	77.6	38.8
F3 (10 kDa-30 kDa)	88.6	44.3
F4 (<10kDa)	8.8	4.4

Although ultrafiltration fractions are based on apparent size of HA substances, TOC results demonstrates the great size difference of used HA compared to the target compound with molecular size of 206 Da. Fraction test was conducted to both provide an analytical basis of size-distribution of competing organic. Also well separated fractions with known size range can be used as well-defined co-existing contaminants in photocatalytic experiment.

To evidence the photocatalytic results from previous experiment a set of similar experiments were conducted using particles with best selectivity (P_3) and different fraction size of HA. Figure 3.16 (c) shows photocatalytic activity when whole the fractions of HA are present. As shown earlier a considerable portion of un-fractioned HA have an apparent molecular size of less than 6 nm. As shown in figure 3.16 (c), presence of small sized molecules results in decline in selectivity of P_3, implying the fact that most of selectivity enhancement was achieved through physical restraining of HA. Similar set of experiments were conducted using smallest fraction of HAs as illustrated in figure 3.16 (d). In agreement with size-exclusion hypothesis, as size of competing organics reduces, selectivity declines. Although still the particles exhibit some selectivity compared to non-porous particles.

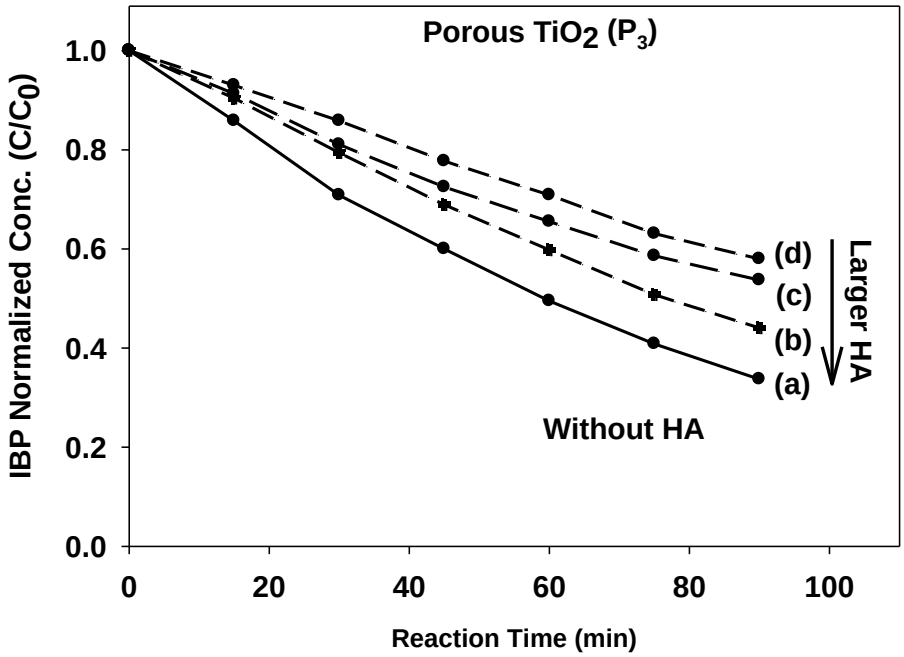

Figure 3.16 Photocatalytic Degradation of Ibuprofen Using Porous (P_3) a) Without HA, b) F_4 Fraction of HA c) Whole Fractions of HA, d) F_1 Fraction of HA

The photocatalytic results along with size-distribution of HA, suggest that physical access of HA was successfully restrained through size-exclusion mechanism. This approach is believed to be applicable concerning significant molecular size difference between target contaminants and NOM present in water. It is also noticeable that porous TiO_2 particles have a much greater surface area compared to non-porous particles which is attractive from activity viewpoint. Also greater surface area provides more adsorption sites for photocatalytic adsorption.

CHAPTER 4

RECOMMENDATIONS AND PROSPECTS

The ultimate aim of this study is to make TiO_2 photocalysis a viable way for photocatalytic decomposition of water contaminants. In this regard selective decomposition of target contaminants is a critical step for utilization of this technology. In water treatment resources we are mostly dealing with a relatively high concentration of NOM along with trace level toxic water contaminants. Although results showed partial improvements in selectivity of TiO_2 nanoparticles using proposed approach, achieving optimum point in selectivity requires extensive research works on synthesize methods. Also a substantial amount of research needs to be done using different combinations of target/competing compounds to validate the efficiency of system for their selective behavior.

4.1 Examination of UV-adsorption Capacity and Recombination Properties of Porous TiO2 Nanoparticles

To obtain an additional insight into photocatalytic activity of porous TiO_2 material, a comprehensive study can be proposed to investigate the effect of void structure on UV-adsorption capacity of different titania material. The intensity of irradiated and reflected UV can be used to estimate the UV utilization of suspension. Comparison between UV utilization of different particles, correlated with their overall activity can demonstrate the overall rate of HRs generation. Also a better understanding of recombination properties of different TiO_2 structures can be achieved by interpreting the UV utilization rate and their overall activity. recombination and their UV to suspension and its change over and reflected UV UV utilization as the only driving force for generation of reactive radicals can be performed through measuring the intensity of irradiated UV adsorbed and transferred to suspended particles. Since UV adsorption is the driving force for generation of active radicals, investigation of UV-adsorption capacity of fabricated TiO2 can be proposed in next mechanism of UV utilization as driving force of HRs generation and recombination of electron/holes as parallel Lower observed activity of porous TiO2 nanoparticles despite their greater BET surface area, implies

4.2 Synthesize of Well-defined Porous TiO_2 Photocatalysts

In this study results from material characterization part demonstrated a relatively wide pore size distribution in porous nanoparticles. Hypothetically the best results could be achieved with extremely narrow pore size distribution. Other synthesizes methods using different procedures or different templating agents can be considered in the next phase of study aimed at narrowing down the throat size distribution of porous network. Also effect of calcination parameters which is believed to have a crucial role in ultimate characteristics of fabricated TiO_2 should be investigated.

4.3 Detailed Study on Photocatalytic Decomposition of Species

To achieve a deeper insight into preferential adsorption of species during the reaction, a further amount of experiments can be proposed using competing organic with extremely well-defined molecular size. Polyethylene glycol (PEG) with defined size can be used as competing agent. The breakdown and decomposition of target and competing compounds can be monitored using zeta sizer during the experiment. Ideally in particles with the best selectivity the average molecular size of PEG remains almost constant during the experiment, indicating their suppression from participating in photocatalytic decomposition. In this study target contaminant was fixed, however real case is usually comprised of a mixture of different contaminants with different molecular size. Similar experiments on different compounds with various hydrophilic characteristics can be proposed.

4.4 Coupling Size-exclusion with Other Methods

As demonstrated in this study, porous TiO_2 nanoparticles with extremely higher surface area can be synthesized thorough templating approach. The provided surface area can serve as an implementation site for previously established strategies such as over-coating and encapsulating. In a novel research work porous TiO_2 nanoparticles can be encapsulated in a porous structure of SiO_2 with extremely well-defined pore size. In the current encapsulated, non-porous TiO_2 nanoparticles, coverage of grain boundary with inactive SiO_2 coating which can significantly decrease accessibility of target compounds to catalyst surface. Despite non-porous particles, the synthesized particles exhibited a great internal active surface for adsorption target species. Synergic effect of selectivity using porous SiO_2

coating and porous structure along with sufficient adsorption sites on the porous-TiO_2 can be beeficial in terms of activity and selectivity, which requires to be examined through experiments.

REFERENCES

[1] M.G. Antoniou, A.A. de la Cruz, D.D. Dionysiou, Cyanotoxins: New generation of water contaminants. J. Environ. Eng. 131(2005) 1239−1243.

[2] M.J. Benotti, R.A. Trenholm, B.J. Vanderford, S.A. Snyder, Pharmaceuticals and endocrine disrupting compounds in U.S. drinking water. Environ. Sci. Technol. 43(2009) 597−603.

[3] U.S. Environmental Protection Agency Office of Water (4303T) Engineering and Analysis Division, Treating Contaminants of Emerging Concern, 2010.

[4] P. Westerhoff, Y. Yoon, S. Snyder, E. Wert, Fate of endocrine-disruptor, pharmaceutical, and personal care product chemicals during simulated drinking water treatment processes. Environ. Sci. Technol. 39 (2005) 6649−6663.

[5] S. Esplugas, D.M. Bila, L.G.T. Krause, M. Dezotti, Ozonation and advanced oxidation technologies to remove endocrine disrupting chemicals (EDCs) and pharmaceuticals and personal care products (PPCPs) in water effluents. J. Hazard. Mater. 149 (2007) 631−642.

[6] J. Yuanhui , Y. Zhuhong , J. Xiaoyan , F. Xin , H. Wenjuan , L. Chang , L. Wei, L. Xiaohua, Thermodynamic Analysis on the Mineralization of Trace Organic Contaminants with Oxidants in Advanced Oxidation Processes, *Ind. Eng. Chem. Res.*, 48 (2009) 10728–10733.

[7] C. von Sonntag, Advanced oxidation processes: mechanistic aspects, Water Science & Technology, 58 (2008) 1015–1021.

[8] G. R. Peyton, Modeling Advanced Oxidation Processes for Water Treatment, Emerging Technologies in Hazardous Waste Management, 7 (1990) 100-118.

[9] R. Munter, Advanced oxidation processes – Current status and prospects. Proc. Estonian Acad. Sci. Chem., Chemistry, 50 (2001) 59-80.

[10] TECHCOMMENTARY: Advanced Oxidation Processes for Treatment of Industrial Wastewater. An EPRI Community Environmental Center Publ. No. 1, 1996.

[11] J.H. Carey, An introduction to AOP for destruction of organics in wastewater. Water Pollut. Res. J. Can., 27 (1992) 1–21.

[12] C.P. Huang, C. Dong, Z. Tang, Advanced chemical oxidation: its present role and potential future in hazardous waste treatment. - Waste Management, 13 (1993) 361-377.

[13] K. Westphal, R. Saliger, D. Jäger, L. Teevs, U. Prüße, Degradation of Clopyralid by the Fenton Reaction, Ind. Eng. Chem. Res. Web publication 2013.

[14] G. Kenanakis, Z. Giannakoudakis, D. Vernardou, C. Savvakis , N. Katsarakis, Photocatalytic degradation of stearic acid by ZnO thin films and nanostructures deposited by different chemical routes, Catal. Today, 151 (2010) 34–38.

[15] S. Rehman, R. Ullah, A. M. Butt , N. D. Gohar, Strategies of making TiO_2 and ZnO visible light active J. Hazard. Mater., 170 (2009) 560–569.

[16] J. Han, W. Qiu , W. Gao, Potential dissolution and photo-dissolution of ZnO thin films, J. Hazard. Mater., 178 (2010) 115-122.

[17] S. W. Y. Wong, P. T. Y. Leung, A. B. Djurišić , K. M. Y. Leung, Toxicities of nano zinc oxide to five marine organisms: influences of aggregate size and ion solubility, Anal. Bioanal. Chem., 396 (2010) 609–618.

[18] T. K. Townsend, E. M. Sabio, N. D. Browning, F. E. Osterloh, Photocatalytic water oxidation with suspended alpha-Fe2O3 particles-effects of nanoscaling, Energy Environ. Sci., 4 (2011) 4270-4275.

[19] H. Choi, S. R. Al-Abed, D. D. Dionysiou, E. Stathatos and P. Lianos, in I. C. Escobar and Andrea Schafer, Eds., Sustainable Water for the Future Water Recycling Versus Desalination, Elsevier B.V. Amsterdam, Netherlands, 2009, 229–254.

[20] P. R. Mishra , O. N. Srivastava, On the synthesis, characterization and photocatalytic applications of nanostructured TiO_2 ,Bull. Mater. Sci., 31 (2008) 545–550.

[21] M. Kaneko, I. Okura, Photocatalysis scince and technology, Springer 2003.

[22] M. Landmann, E. Rauls, W. G. Schmidt, The electronic structure and optical response of rutile, anatase and brookite TiO_2, J. Phys.: Condens. Matter 24 (2012) 1-6.

[23] K. Vinodgopal, D.E. Wynkoop, P.V. Kamat, Environmental Photochemistry on semiconductor surfaces: A photosensitization approach for the degradation of a textile azo dye, Acid Orange 7. Environ. Sci. Technol., 30 (1996) 1660-1666.

[24] J. Blanco, P. Avila, A. Bahamonde, E. Alvarez, B. Sanchez, M. Romero, Photocatalytic destruction of Toluene and Xylene at gas-phase on a titania based monolithic catalyst. Catal Today., 29 (1996) 437-442.

[25] Y. Mao, Y., A. Bakac, Photocatalytic Oxidation of Aromatic Hydrocarbons. Inorg. Chem., 35 (1996) 3925-3930.

[26] I.W. Huang, C.S. Hong, B. Bush, Photocatalytic degradation of PCBs in TiO_2 aqueous suspensions. Chemosphere, 32 (1996) 1869-1881.

[27] F. Gianturco, C.M. Chiodaroli, I.R. Bellobono, M.L. Raimondi, A. Moroni, B. Gawlik, Pilot-plant photomineralization of atrazine in aqueous solution by photocatalytic membranes immobilising titanium dioxide and promoting photocatalysts. Fresenius Environ. Bull., 6 (1997) 461-468.

[28] C. Minero, E. Pelizzetti, S. Malato, S., J. Blanco, Large solar plant photocatalytic water decontamination: degradation of atrazine. Solar Energy, 56 (1996) 411-419.

[29] J. Lobedank, E. Bellmann, J. Bendig, Sensitized photocatalytic oxidation of herbicides using natural sunlight. J. Photochem. Photobiol. A:Chem., 108 (1997) 89-93.

[30] M.M. Haque, M. Muneer, Heterogeneous photocatalysed degradation of a herbicide derivative, isoproturon in aqueous suspension of titanium dioxide. J.Environ. Manag., 69 (2003) 169-176.

[31] M. Muneer, D. Bahnemann, Semiconductor mediated photocatalysed degradation of two selected pesticide derivatives, terbacil and 2,4,5-tribromoimidazole in aqueous suspension. Appl. Catal. B: Environ., 36 (2002) 95-111.

[32] D.C. Schmelling, K.A. Gray, P.V. Kamat, The role of reduction in the photocatalytic degradation of TNT. Environ. Sci. Technol., 30 (1996) 2547-2555.

[33] N.N. Rao, S. Dube, Photocatalytic degradation of mixed surfactants and some commercial soap/detergent products using suspended TiO_2 catalysts. J. Mol. Catal. A:Chem., 104 (1996) 197-199.

[34] I. Liu, L.A. Lawson, B. Cornish, P.K.J. Robertson, Mechanistic and toxicity studies of the photocatalytic oxidation of microcystin-LR. J. Photochem. Photobiol. A:Chem., 148 (2002) 349-354.

[35] B.V. Mihaylov, J.L. Hendrix, J.H. Nelson, Comparative catalytic activity of selected metal oxides and sulphides for the photo-oxidation of cyanide. J. Photochem. Photobiol. A:Chem., 72 (1993) 173-177.

[36] S.N. Frank, A.J. Bard, A.J., Heterogeneous photocatalytic oxidation of cyanide and sulfite in aqueous solutions at semiconductor powders. J. Phys. Chem., 81 (1977) 1484-1488.

[37] R.B. Draper, M.A. Fox, Titanium dioxide photooxidation of thiocyanate:(SCN)2.cntdot.- studied by diffuse reflectance flash photolysis. J. Phys. Chem., 94 (1990) 4628-4634.

[38] A. Bravo, J. Garcia, X. Domenech, J. Peral, Some observations about the photocatalytic oxidation of cyanate to nitrate over TiO_2. Electrochim. Acta, 39 (1994) 2461-2463.

[39] A. Mills, S. Le Hunte, An overview of semiconductor photocatalysis. J. Photochem. Photobiol. A:Chem., 108 (1997) 1-35.

[40] M. Bissen, M. M. Vieillard-Baron, A. J. Schindelin, F. H. Frimmel, TiO_2-catalyzed photooxidation of arsenite(III) to arsenate(V) in aqueous samples Chemosphere 44 (2001) 751-757.

[41] B. Neppolian, E. Celik, H. Choi, Photochemical Oxidation of Arsenic(III) to Arsenic(V) using Peroxydisulfate Ions as an Oxidizing Agent, Environ. Sci. Technol. 42 (2008) 6179-6184.

[42] L.R. Skubal, N.K. Meshkov, Reduction and removal of mercury from water using arginine-modified TiO_2, J. Photochem. Photobiol., A , 148 (2002) 211–214.

[43] B. Deng, A.T. Stone, Surface-catalyzed chromium(VI) reduction: The TiO_2–Cr(VI)–mandelic acid system, Environ. Sci. Technol., 30 (1996) 463-472 .

[44] H. Choi, S.R. Al-Abed, D.D. Dionysiou, E. Stathatos, P. Lianos, TiO_2-based advanced oxidation nanotechnologies for water purification and reuse, pp. 229–254, in: Sustainability Science and Engineering, Volume 2: Sustainable Water for the Future (Eds. Isabel I. Escobar and Andrea I. Schafer); Elsevier Science: Netherlands, 2009.

[45] E. Brillasa, E. Mur, R. Sauleda, L. Sanchez, J. Peral, X. Domenech, J. Casado, Aniline mineralization by AOP's: Anodic oxidation, photocatalysis, electro-Fenton and photoelectro-Fenton processes. Appl. Catal. B, 16 (1998) 31−42.

[46] T.E. Doll, F.H. Frimmel, Photocatalytic degradation of carbamazepine, clofibric acid and iomeprol with P25 and Hombikat UV100 in the presence of natural organic matter (NOM) and other organic water constituents, Water Res., 39 (2005) 403-411.

[47] H. Choi, S.R. Al-Abed, Effect of reaction environments on the reactivity of PCB (2-chlorobiphenyl) over activated carbon impregnated with palladized iron, J. Hazard. Mater., 179 (2010) 869-874.

[48] N.Z. Muradov, A. T-Raissi, D. Muzzey, C.R. Painter, M.R. Kemme, Selective photocatalytic destruction of airborne VOCs, Solar Energy, 56 (1996) 445-453.

[49] Y. Paz, Preferential photodegradation - why and how? C.R. Chimie, 9 (2006) 774–787.

[50] K.H. Wang, Y.H. Hsieh, L.J. Chen, The heterogeneous photocatalytic degradation, intermediates and mineralization for the aqueous solution of cresols and nitrophenols, J. Hazardous Mater. 59 (1998) 251-260.

[51] J. Augustinski, Structural Bonding, Springer, Berlin, New York, 1988, p. 69.

[52] A. Fernandez- Nieves, C. Richter, F.J. de las Nieves, Point of zero charge estimation for a TiO_2/water interface Prog. Colloid Sci., 110 (1998) 21-24.

[53] L.A.G. Rodenas, A.D. Weisz, G.E. Magaz, M.A. Blesa, Effect of light on the electrokinetic behavior of TiO_2 particles in contact with Cr(VI) aqueous solutionsJ. Colloid Interface Sci. 230 (2000) 181-185.

[54] J. Chen, D.F. Ollis,W.H. Rulkens, H. Bruning, PHOTOCATALYZED OXIDATION OF ALCOHOLS AND ORGANOCHLORIDES IN THE PRESENCE OF NATIVE TiO_2 AND METALLIZED TiO_2 SUSPENSIONS. PART (I):, PHOTOCATALYTIC ACTIVITY AND pH INFLUENCE, Water Res. 33 (1999) 661-668.

[55] K. Inumaru, M. Murashima, T. Kasahara, S. Yamanaka, Enhanced photocatalytic decomposition of 4-nonylphenol by surface-organografted TiO_2: a combination of molecular selective adsorption and photocatalysis Appl. Catal. B: Environ. 52 (2004) 275-280.

[56] R. Rudolph, K.P. Francke, H. Miessner, OH Radicals as Oxidizing Agent for the Abatement of Organic Pollutants in Gas Flows by Dielectric Barrier Discharges, Plasmas and Polymers, 8 (2003) 153-161.

[57] M.F. Rahman, E.K. Yanful, S.Y. Jasim, Endocrine disrupting compounds (EDCs) and pharmaceuticals and personal care products (PPCPs) in the aquatic environment: implications for the drinking water industry and global environmental health. J. Water Health 7 (2009) 224−243.

[58] P. Westerhoff, Y. Yoon, S. Snyder, E. Wert, Fate of endocrine-disruptor, pharmaceutical, and personal care product chemicals during simulated drinking water treatment processes. Environ. Sci. Technol., 39 (2005) 6649−6663.

[59] Larry L. Hench , Jon K. West, The sol-gel process, Chem. Rev., 90 (1990) 33–72.

[60] By Jin Ho Bang and Kenneth S. Suslick, Applications of Ultrasound to the Synthesis of Nanostructured Materials, Adv. Mater., 22 (2010) 1039–1059.

[61] J. N. Israelachvili , D. J. Mitchell, B. W. Ninham, Theory of self-assembly of hydrocarbon amphiphiles into micelles and bilayers, J. Chem. Soc., Faraday Trans. 2, 72 (1976) 1525-1568.

[62] R. Nagarajan , E. Ruckenstein, Theory of Surfactant Self -Assembly: A Predictive Molecular Thermodynamic Approach Langmuir, 7 (1991) 2934–2969.

[63] H. Choi, E. Stathatos , D. D. Dionysiou, Sol-gel preparation of mesoporous photocatalytic TiO_2 films and TiO_2/Al_2O_3 composite membranes for environmental applications, Appl. Catal., B, 63 (2006) 60–67

[64] H. Buser, T. Poiger, M. Muller, Occurence and environmental behavior of the chiral pharmaceutical drug ibuprofen in surface waters and in wastewater; Environ. Sci. Technol. ; 33 (1999)15:2529.

[65] N. Vieno, T. Tuhkanen, L. Kronberg, Seasonal variation in the occurence of pharmaceuticals in effluents from a sewage treatment plant and in the recipient water; Environ. Sci. Technol. ,39 (2005) 8220 .

[66] C. Zwiener, F. Frimmel, Oxidative treatment of pharmaceuticals in water; Water Research ; 34 (2000) 1881.

[67] C.G. Daughton, Pharmaceutical Ingredients in Drinking Water: Overview of Occurrence and Significance of Human Exposure, by US-EPA.

[68] S.M. Chauhan, B. B. Sahoo, Biomimetic oxidation of ibuprofen with hydrogen peroxide catalysed by horseradish peroxidase (HRP) and 5,10,15,20-tetrakis-(2',6'-dichloro-3'-

sulphonatophenyl)porphyrinatoiro n(III) and manganese(III) hydrates in AOT reverse micelles. Bioorg Med Chem. 7 (1999) 2629-2634.

[69] USEPA, http://water.epa.gov/lawsregs/rulesregs/sdwa/chemicalcontaminantrules/upload/FR1-30-91.pdf (accessed 15 March 2013)

[70] P. Rajanikant , P. Nirav, N.M. Patel, M.M. Patel, A novel approach for dissolution enhancement of Ibuprofen by preparing floating granules, Int. J. Res. Pharm. Sci., 14 (2010) 57-64.

[71] S.T. Nishanthia, D. H. Rajac, E. Subramanianb, D. P. Padiyan, Remarkable role of annealing time on anatase phase titania nanotubes and its photoelectrochemical response, Electrochimica Acta, 89 (2013) 239–245.

[72] H. Choi, A. C. Sofranko, D. D. Dionysiou, Nanocrystalline TiO_2 Photocatalytic Membranes with a Hierarchical Mesoporous Multilayer Structure: Synthesis, Characterization, and Multifunction, Adv. Funct. Mater., 16 (2006) 1067–1074.

[73] D.C. William, Materials Science and Engineering: An Introduction; John Wiley and Son, Inc.: New York, 2003.

[74] J. Yang, J.M.F. Ferreira, On the Titania Phase Transition by Zirconia Additive in a Sol-Gel-Derived Powder Mater. Lett., 36 (1998) 389-394.

[75] D.A. Reckhow, P.C. Singer, R.L. Malcolm, Chlorination of humic materials: Byproduct formation and chemical interpretations. Environmental Science and Technology 24 (1990) 1655–1664.

[76] K. Ghosh, M., Schnitzer, Macromolecular structures of humic substances. Soil Science, 129 (1980) 266–276.

[77] A. Piccolo, S. Nardi, G. Concheri, Micelle-like conformation of humic substances as revealed by size exclusion chromatography. Chemosphere, 33 (1996) 595–602.

[78] A. Piccolo, P. Conte, A. Cozzolino, Effects of mineral and monocarboxylic acids on the molecular association of dissolved humic substances. European Journal of Soil Science 50 (1999) 687–694.

[79] A. Piccolo, P. Conte, E. Trivellone, B. van Lagen, P. Buurman, Reduced heterogeneity of a lignite humic acid by preparative HPSEC following interaction with an organic acid. Characterization of

size-separates by Pyr-GC-MS and1 H-NMR spectroscopy. Environmental Science and Technology 36 (2002) 76–84.

[80] Stevenson F.J.: Humus chemistry genesis, composition, reactions. Willey Interscience, New York 1982.

BIOGRAPHICAL INFORMATION

Abolfazl Zakersalehi was born 1987 in Tehran, Iran. He earned his bachelor degree in civil engineering at Sharif University of Technology (SUT) at 2005. At SUT he was an active member of environmental organizations. He started his master degree in environmental engineering at the University of Texas at Arlington (UTA) in 2011. During his master degree, he held different teaching and research assistantship positions regarding water treatment processes. His research works mainly focuses on novel approaches for water purification including nanotechnology-enabled water treatment.